UCRL-18642

cy. 2

STUDIES OF THE SUBLIMINATION MECHANISM OF SOLIDS

RECEIVED
LAWRENCE
RADIATION LABORATORY

JAN 22 1969

LIBRARY AND
DOCUMENTS SECTION

G. A. Somorjai

December 1968

TWO-WEEK LOAN COPY

This is a Library Circulating Copy
which may be borrowed for two weeks.
For a personal retention copy, call
Tech. Info. Division, Ext. 5545

UCRL-18642

cy. 2

LAWRENCE RADIATION LABORATORY
UNIVERSITY of CALIFORNIA BERKELEY

DISCLAIMER

This document was prepared as an account of work sponsored by the United States Government. While this document is believed to contain correct information, neither the United States Government nor any agency thereof, nor the Regents of the University of California, nor any of their employees, makes any warranty, express or implied, or assumes any legal responsibility for the accuracy, completeness, or usefulness of any information, apparatus, product, or process disclosed, or represents that its use would not infringe privately owned rights. Reference herein to any specific commercial product, process, or service by its trade name, trademark, manufacturer, or otherwise, does not necessarily constitute or imply its endorsement, recommendation, or favoring by the United States Government or any agency thereof, or the Regents of the University of California. The views and opinions of authors expressed herein do not necessarily state or reflect those of the United States Government or any agency thereof or the Regents of the University of California.

Submitted to Advances in
High Temperature Chemistry,
Vol. II.

UCRL-18642
Preprint

UNIVERSITY OF CALIFORNIA

Lawrence Radiation Laboratory
Berkeley, California

AEC Contract No. W-7405-eng-48

STUDIES OF THE SUBLIMATION MECHANISM OF SOLIDS

G. A. Somorjai

December 1968

TABLE OF CONTENTS

I. INTRODUCTION 1

II. PRINCIPLES OF VAPORIZATION STUDIES 3

III. EXPERIMENTAL CONSIDERATIONS 7

IV. STUDIES OF THE SUBLIMATION MECHANISM OF SODIUM CHLORIDE SINGLE CRYSTALS 9

A. Effect of Dislocations on the Evaporation Rate 10

B. Effect of Divalent Impurities (Ca^{2+}) on the Evaporation Rate 12

C. Discussion 13

V. STUDIES OF THE SUBLIMATION MECHANISM OF CADMIUM SULFIDE SINGLE CRYSTALS 17

A. Effect of Doping of CdS on its Evaporation Rate 17

B. The Effect of Light on the Evaporation Rate of CdS 19

C. Surface Concentration Dependence of the Evaporation Rate of CdS 20

VI. STUDIES OF THE SUBLIMATION MECHANISM OF GALLIUM ARSENIDE SINGLE CRYSTALS 23

A. Results 24

B. Mass Spectrometric Studies 25

C. Effect of Liquid Gallium on the Vaporization of GaAs . . . 27

D. Discussion 27

VII. LOW ENERGY ELECTRON DIFFRACTION (LEED) STUDY OF THE VAPORIZING SILVER (100) SURFACE 30

VIII. CONCLUSIONS 34

A. Composition of the Surface 34

B. Charge Transfer 34

C. Impurities 35

D. Concurrent Vaporization Mechanisms 35

E. Invariance of Vapor Composition 36

ACKNOWLEDGEMENTS 36

REFERENCES 37

TABLES 41

FIGURE CAPTIONS 43

FIGURES 45

I. INTRODUCTION

Investigations of the chemical reactions which control the vaporization of solids has become one of the most rapidly growing fields of thermochemistry. In these studies the vaporization rates and vapor compositions of solids are measured far from equilibrium, in order to obtain information about their kinetics of sublimation (Somorjai and Lester, 1967). Vaporization takes place under non-equilibrium conditions for most systems of technological importance. It is only reasonable to assume that an understanding of the kinetics and mechanism by which the vaporizing species break away from the surface of the condensed phase will permit one to control the rate of vaporization, reduce or increase it, as desired.

The vaporization rate of many solids into vacuum have already been found to be much smaller than the maximum vaporization rate which can be calculated from equilibrium vapor pressure data (Somorjai and Lester, 1967). For many solids (As [Brewer and Kane, 1955], P [Kane 1955], GaAs) the presence of liquid metals on the vaporizing surface may increase the sublimation rate by orders of magnitude to that of the maximum rate. For other solids (NaCl [Lester and Somorjai, 1968], CdS [Somorjai and Lyon, 1965] the presence of trace impurities (in part per million quantities) or small changes in defect concentration can decrease the sublimation rates by orders of magnitude. All of these striking changes in the vaporization rates are due to changes in the vaporization mechanism. By making minute changes in the composition of the vaporizing solid or in the conditions of sublimation we may change the rate limiting reaction step in a series of reactions (Somorjai and Lester, 1967) which finally

lead to the desorption of the vaporizing species.

Recent studies of vaporization have uncovered a great deal of information about the vaporization mechanism of different monatomic and diatomic solids (Somorjai, 1968a; Rosenblatt and Lee, 1968). It is hoped that as more materials will be investigated we shall be able to identify the important structural or electronic parameters which are controlling the sublimation process. We can then use this information to develop a unified theory of vaporization which can be used to predict vaporization mechanisms for different groups of materials.

We have been studying the vaporization characteristics of several solids to obtain information about the relationship between their chemical bonding and their sublimation mechanism. For these investigations we have selected binary compounds from groups IA-VIIA, IIB-VIA and IIIA-VA in the periodic table. In this paper we shall discuss and compare the sublimation characteristics of sodium chloride, cadmium sulfide and gallium arsenide. It is hoped that other compounds with similar bonding characteristics have similar vaporization mechanisms.

II. PRINCIPLES OF VAPORIZATION STUDIES

Consider a perfectly flat face of a monatomic single crystal in which the binding energies of all surface atoms are equal to each other. Since all atoms in such a crystal face have equal probability to vaporize the overall evaporation rate is given by (Somorjai and Lester, 1967)

$$J^{v}_{max}\ (\text{moles/cm}^2\text{sec}) = k_v\ (A)_s^{max} \qquad (1)$$

where k_v is the rate constant of the vaporization reaction and $(A)_s^{max}$ is the total concentration of surface atoms. The maximum rate of condensation of the vapor flux on such a face is given by

$$J^{c}_{max}\ (\text{moles/cm}^2\text{sec}) = k_c(A)_g = (RT/2\pi M_A)^{1/2}\ (A)_g \qquad (2)$$

where $(A)_g$ is the vapor density, R is the gas constant, T is the absolute temperature and M_A is the atomic weight of $(A)_g$. In equilibrium, the vaporization and condensation rates are equal $[k_v(A)_s = k_c(A)_g]$. Thus, the evaporation rate can be expressed in terms of the condensation rate and the well-known equation (Hertz, 1882; Knudsen, 1915; Langmuir, 1913)

$$J^{v}_{max}\ (\text{moles/cm}^2\text{sec}) = P_{eq}\ (2\pi M_A RT)^{-1/2} \qquad (3)$$

is obtained assuming the ideal gas law. If the condensation rate is smaller than the evaporation rate due to external "pumping" there is a net rate of removal, R, of vapor flux from the vaporizing surface which is given by

$$R = J^{v} - J^{c} \qquad (4)$$

In equilibrium the net rate is zero (R = 0) and for vaporization into

vacuum, $R = J^V$.

Now let us consider a "real" surface, in which there are many atomic positions. These are distinguishable by their different numbers of nearest neighbors. Surface atoms have different binding energies depending on which atomic positions they occupy. Under these conditions, only a small fraction of the total number of surface atoms will occupy positions of lowest binding energy from which vaporization can most readily proceed. We may rewrite Eq. (1) as

$$J^V \text{ (moles/cm}^2 \text{ sec)} = k_o \, (A)_s \exp(-E^*/RT) \qquad (5)$$

where $(A)_s$ is the concentration of atoms in surface sites from which vaporization takes place, k_o is a constant related to the frequency of attempted motion of vaporizing molecules over the energy barrier, E^*. Thus, the evaporation rate of a "real" crystal surface can be different from the evaporation rate of a "homogeneous" surface due to variations of the surface concentration $(A)_s$ or on account of a different activation energy of vaporization, E^*. If the concentration of surface sites from which vaporization can occur is smaller than the total concentration of surface atoms, $[(A)_s < (A)_s^{max}]$, the evaporation rate will be smaller than if all surface atoms could vaporize with equal probability.

A heterogeneous surface however has many atomic ledges and steps and exhibits "roughness" on an atomic scale. Therefore surface area of a "real" crystal could be appreciably larger than the geometrical surface area. Although not every surface atom may have low enough binding energy to vaporize the concentration of those which vaporize can be sufficiently greater on a rough surface than on a "homogeneous"

surface. Melville (1936) and Winterbottom (1966) have shown that no matter how rough the surface becomes the evaporation rate may reach but cannot exceed the maximum sublimation rate from a crystal with the smooth geometrical surface area (if the condensation rates are near to maximum). Thus, the surface concentration of atoms of weakest binding energy in a "real" surface may increase and become equal to the surface density of atoms in a homogeneous surface. The vacuum evaporation rate would simultaneously increase until the maximum rate, J^V_{max}, is reached.

It is customary (Somorjai and Lester, 1967) to express the deviation of the vacuum evaporation rate, J^V, from the maximum, equilibrium rate, J^V_{max} in terms of the evaporation coefficient, α, which is given by,

$$\alpha(T) = J^V (T)/J^V_{max} (T) \qquad (6)$$

If the vacuum evaporation rate is equal to the maximum rate, $\alpha(T) = 1$, of if $J^V \ll J^V_{max}$, $\alpha(T) \ll 1$.

The activation energy of vaporization, E^*, can be larger or smaller than the equilibrium heat of vaporization, ΔH_v, or can be equal to it. Its magnitude reflects the overall energy necessary for the surface atoms to participate in the rate limiting reaction step (or steps) (Somorjai and Lester, 1967). Vaporization is a multi-step process in which atoms break away from their lattice sites, may diffuse on the surface until they are ready to vaporize. For many solids the surface atoms must undergo rearrangements such as association, dissociation or charge transfer prior to desorption from the vaporizing surface (Somorjai and Lester, 1967). The rate of any of these reaction steps may control the overall sublimation process. Certain solids may vaporize by two different reaction paths

which can operate simultaneously at different surface sites (Lester and Somorjai, 1968).

The activation energy of vaporization may change as the experimental vaporization conditions are varied. In order to be able to compare activation energies of different sublimation reactions, values, which are often listed (Somorjai and Lester, 1967) are determined from measurements using the pure solids and are carried out in vacuum ($J^c = 0$; $R = J^v$).

III. EXPERIMENTAL CONSIDERATIONS

The experimental techniques which are most frequently used in sublimation studies are 1) total weight loss measurements using microbalance or torsion balance and 2) mass-spectrometric studies of the composition of the vapor flux. The two techniques are complementary; weight loss measurements give absolute evaporation rates. From these studies, as a function of temperature, the activation energy of vaporization (per mole of solid) is determined. Mass spectrometric investigation of the vapor flux allows one to determine and monitor the vapor composition. The activation energies of vaporization (per mole of vapor) of each vaporizing species can be calculated from the variation of the composition with temperature. Typical microbalance and mass spectrometer systems which are used in our vaporization studies (Lester and Somorjai, 1968) are shown in Figs. 1 and 2.

For purposes of definitive studies of sublimation mechanisms one face of a single crystal should be used. Evaporation rates obtained using polycrystalline samples are very difficult to interpret due to their unknown free surface area (Brewer and Kane, 1955; Rosenblatt, 1963). These samples contain a large inner surface from which the vaporizing atoms will undergo many collisions before leaving the solid. Thus, a certain fraction of the powder surface acts as an equilibrium source.

The crystal face which is to be used in the sublimation studies should be well characterized. It should be a "stable" surface which retains its crystallographic orientation throughout the experiments (Somorjai and Stemple, 1953). It is important to determine its dislocation density using etch-pit count techniques (Lester and Somorjai, 1968) and

to investigate its surface topology using optical or electron microscopy (Searcy, 1968). It has been shown that the surface structure can markedly influence the evaporation rates of many solids (Lester and Somorjai, 1968; Rosenblatt and Lee, 1968; Searcy, 1968). The bulk properties of the vaporizing crystal samples should also be well characterized. There is, in general, communication between the bulk and the vaporizing surface via atom or defect diffusion or via charge transfer (Somorjai and Lester, 1967; Somorjai and Lyon, 1965). Thus, changes in bulk properties may greatly influence the evaporation rate. The defect, impurity and charge concentrations in the bulk solid should be determined.

Since the structure, composition and other physical chemical properties of both, the surface and the bulk depend on the thermal history of the solid, it is necessary to devise a suitable heat treatment to standardize these parameters at the onset of the vaporization studies (Somorjai and Lester, 1967 ; Somorjai and Lester, 1965a).

Several additional techniques have become available in recent years which can be applied to studies of vaporization kinetics. These include low energy electron diffraction (Morabito and Somorjai, 1968), Auger spectroscopy (Palmberg and Rhodin, 1968), ellipsometry (Morabito, et al., 1968), and scanning electron microscopy (Searcy, 1968).

IV. STUDIES OF THE SUBLIMATION MECHANISM OF SODIUM CHLORIDE SINGLE CRYSTALS

Sodium chloride vaporizes according to the dominant net reaction (Lester and Somorjai, 1968; Berkowitz and Chupka, 1958)

$$NaCl(solid) \rightarrow (1-x)NaCl(vapor) + x/2\ Na_2Cl_2(vapor) \quad .$$

In the temperature range of our investigation, 450° to 650°C, and under the different vaporization conditions, the dimer is roughly 5-30 mole percent of the vapor.

The majority of the crystals used in these vaporization studies were obtained from the Harshaw Chemical Company. These crystals are 99.95% pure. The major impurities are anions containing bromine and oxygen (probably Br^-, OH^- and O_2^-). Polyvalent cation impurities were present at levels not exceeding 5 ppm.

Dislocation densities were determined by counting chemically formed etch pits on a (100) cleavage face which was used in all of the vaporization studies. Most of the pure NaCl crystals had etch pit densities of $0.8 - 4\times10^6/cm^2$. We have assumed a constant proportionality between observed etch pits and dislocations which intersect the surface under observation and that the proportionality factor is close to one. The dislocation density of a crystal could be increased by plastically deforming it. Crystals with dislocation densities (etch pit counts) as high as $1.5\times10^7/cm^2$ were produced in this way. Etch pits in the unstrained crystals generally were uniformly distributed; however, in the strained crystals they tended to appear in "slip bands." Therefore, the etch pit density was counted in several areas on the surface and the results averaged to obtain the reported figure for these crystals.

A. Effect of Dislocations on the Evaporation Rate

The (100) face of sodium chloride was used in these studies. This face remained stable throughout the vaporization run, i.e. it did not exhibit faceting to other low index crystal planes. Thus, steady state evaporation rates could readily be obtained at a given temperature. Initial experiments showed large variations in the total evaporation rates from crystal to crystal (factor of three). In every case, however, steady state vaporization rates for a given sample could readily be achieved and maintained. It was discovered that the total evaporation rate of sodium chloride crystals depends on the dislocation density in the sample. Figure 3 shows a plot of the logarithm of the evaporation rates of sodium chloride crystals with two different dislocation densities ($\sim 1\times10^{6}$ cm^{-2} and $\sim 1\times10^{7}$ cm^{-2}) as a function of reciprocal temperature. Here we can also plot the maximum evaporation rate as calculated from equilibrium vapor pressure measurements. The steady state evaporation rate was approximately doubled by increasing the dislocation density by an order of magnitude. Sodium chloride crystals with dislocation densities of $\sim 10^{6}$ cm^{-2} gave evaporation rates which were lower than the equilibrium rate by about a factor of two. The crystals with larger etch pit counts ($\sim 10^{7}$ cm^{-2}) had evaporation rates equal to the maximum equilibrium rate. Except for dislocation density these crystals should be identical (impurities and preparation technique). These curves give an average activation energy of vaporization of approximately 55 kcal/mole. It should be noted that this value is a weighted average of the activation energies of vaporization of the monomer and dimer molecules for the different dislocation density crystals.

The composition of the vapor flux emanating from the subliming (100) crystal face of sodium chloride was monitored by a quadrupole mass spectrometer as a function of temperature. The ion peaks detected in the mass spectrum of sodium chloride vapor were m/e = 23 (Na^+), 58,60 ($NaCl^+$) and 81,83 (Na_2Cl^+). A representative curve showing the logarithm of the ion intensities (Na^+, $NaCl^+$, Na_2Cl^+) as a function of the reciprocal temperature is given in Fig. 4. These slopes were used to calculate the activation energies of vaporization for both NaCl(vapor) and Na_2Cl_2(vapor). We also plot representative values of the computed monomer to dimer ratio on a semilogarithmic scale as a function of temperature.

We have also monitored the vapor composition from the (111) crystal face of sodium chloride as a function of temperature. Within the accuracy of our measurements both the monomer to dimer ratio and the activation energies of vaporization, E_D^* and E_M^* were identical to those for the (100) face of sodium chloride crystals of similar dislocation density. Inspection of the (111) face after the vaporization studies revealed the development of facets of (100) orientation. It is likely that after a short transient the unstable (111) surface has virtually disappeared and the largest fraction of the vapor flux came from the freshly formed (100) facets. In Table I we list the activation energies of vaporization for the monomer and the dimer from crystals of different dislocation density. It is apparent that the activation energies vary somewhat for crystals with different etch pit densities. There seems to be a small increase in the activation energies with increasing dislocation density which is not significantly outside our experimental error. The monomer to dimer ratio appears not to change appreciably with increasing dislocation

density in the crystals. There may be a small increase in the monomer concentration relative to the dimer for the highly strained samples (1×10^7 cm^{-2}).

B. Effect of Divalent Impurities (Ca^{2+}) on the Evaporation Rate

Sodium chloride single crystals containing 330 ± 50 ppm Ca^{2+} ions used in these studies show the effect of divalent impurities on the vacuum evaporation rate of NaCl.* Figure 5 shows the evaporation rates of these crystals as a function of the reciprocal temperature on a semi-logarithmic plot. There is a large decrease of the total evaporation rate (by a factor of five) for crystals doped with calcium. These Ca^{++} doped crystals not only show drastically reduced evaporation rates but also a marked increase of the average activation energy of vaporization. While the average vaporization coefficient has dropped to $\alpha \sim 0.1$ from $\bar{\alpha} \sim 0.5$ obtained for the pure low dislocation density sodium chloride crystals, the average activation energy of vaporization has increased to $\bar{E}^* \simeq 63$ kcal/mole with respect to that obtained for the pure crystals ($\bar{E}^* \simeq 55$ kcal/mole).

There is experimental evidence indicating that the concentration of calcium ions slowly increases at the vaporizing sodium chloride surface as a function of time during vaporization. The evaporation rate was found to decrease slowly for a given sample during the experiment. Simultaneously, the apparent activation energy of vaporization also increases. The vaporization data given in Fig. 5 are representative of the results obtained early in the measurements using several calcium-doped samples.

---

* In addition to Ca^{2+}, sodium ion vacancies in excess of their steady state concentration have also been introduced in the sodium chloride crystal lattice.

Sodium chloride samples doped with Br^- ion showed vaporization characteristics which were identical to undoped high purity single crystals of the same dislocation density. The presence of oxygen or OH^- ions in the crystals also had no observable effect on the evaporation rates in the temperature range of this study.

C. Discussion

We find that the steady state vacuum vaporization rate of the solid is determined by the dislocation density. These results indicate that the dislocation density in the sodium chloride crystals remains largely unchanged throughout the vaporization and that dislocations control the concentration of surface sites from which vaporization is to occur. An order of magnitude increase in the dislocation density increased the evaporation rate by a factor of two or the average evaporation coefficient from $\bar{\alpha} \sim 0.5$ to $\bar{\alpha} \sim 1.0$. The activation energies of vaporization exhibit a small upward trend with increasing dislocation densities and corresponding increased rates of vaporization. This change in activation energy is less than 3 kcal. It should be noted that an increase of two kilocalories in E^* would decrease the evaporation rate of NaCl by a factor of three at 800°K if there were no accompanying changes in the pre-exponential factor. We observed an increase in the rate by a factor of two (2x). Thus the preexponential factor would have to increase by a factor of six to accommodate the increased evaporation rate in this case. It is apparent from our data that an etch pit density of 10^7 cm^{-2} corresponds to a dislocation density sufficient to establish the maximum equilibrium vaporization rate. We cannot say what is the lower limit on the vaporization rate of high purity crystals as we were not able to prepare samples

with dislocation densities lower than $\sim .8 \times 10^6$ cm^{-2}.

The monomer to dimer ratios were essentially unchanged for all of the sodium chloride crystals within the accuracy of the measurement (with the exception of the crystals of the highest dislocation density which showed larger relative monomer concentrations). If the dimers formed by an equilibrium association of two monomer molecules adsorbed on the surface then the monomer to dimer ratio, M/D, should decrease as a function of the increasing monomer concentration, i.e., $M/D \propto 1/M$, at a given temperature. This does not happen. For crystals which have high vaporization fluxes (and high dislocation densities) there are more monomer molecules on the surface, but, if anything, the monomer to dimer ratio increases with respect to the lower vaporization rate crystals (low dislocation density). Thus, there is no equilibrium between the monomer and dimer molecules on the vaporizing sodium chloride surface. It seems that the monomer to dimer ratio is fixed by the relative energies necessary to remove a monomer or dimer, respectively, from a surface site. The absence of any appreciable equilibrium interaction between the absorbed monomer and/or dimer molecules could be due to the short residence time of these molecules on the vaporizing surface prior to desorption into vacuum. The mean free path ($\bar{X}$) of molecules away from the ledge depends on the activation energies of surface diffusion, E^*_{diff}, and of desorption, E_{des}, from the free surface and can be estimated by the equation $\bar{X} = a \exp [(E_{des} - E^*_{diff})/2kT]$ where a is the interatomic distance (Burton et al., 1951). For KCl these energies have been calculated to be $E_{des} = 0.35$ eV and $E^*_{diff} = 0.23$ eV (Hove, 1955). These energies should be similar for NaCl. Using these values, at T = 800°K, we have $\bar{X} = 0.4a$. Thus, at the vaporization

temperature the mean free path of the sodium chloride molecule would not be more than a few lattice spacings. This implies that most of the monomer and dimer molecules vaporize near ledges and that surface diffusion cannot play an important role in the vaporization reaction. The lack of any appreciable surface diffusion also inhibits the establishment of a steady state ledge concentration at the vaporizing surface which could be approximated by the equilibrium value. It is apparent that the removal of a sodium chloride molecule from a surface site became more difficult in the presence of neighboring divalent ions or sodium ion vacancies which are introduced in excess of the steady state concentration. Such a marked effect on the evaporation rate by doubly charged impurities indicates that the breaking away of sodium chloride molecules from lattice sites (kinks) on the vaporizing surface is a rate controlling step.

These vaporization characteristics of the sodium chloride single crystals can be explained in terms of the stepwise model of vaporization of the heterogeneous solid surface (Stranski, 1928). We postulate a possible mechanism of vaporization of sodium chloride which can explain most of the data.

1. Ledges (of approximately monatomic height) are formed in large concentrations at positions where dislocations intersect the surface (and at the edges of the crystal).

2. Both monomer and dimer molecules are formed at the same sites (kinks) on these ledges.

3. The desorption rate of both monomer and dimer molecules from the proximity of the ledges is rapid.

The first step explains the observed increase of the evaporation rate of sodium chloride surfaces with increased density of dislocations. Dislocations have been shown to be nucleation sites for crystal growth and thermal etch pits have been observed on alkali halide crystals at the point of emergence of dislocations at the surface.

The second and third step, the breaking away of both monomer and dimer molecules independently from the kinks and the apparent absence of any surface diffusion explains the insensitivity of the monomer to dimer ratio to increased dislocation density. The marked decrease of the evaporation rate (factor of five) of calcium doped crystals and the simultaneous large increase in the activation energy of vaporization indicate that the breaking away of sodium chloride molecules at ledges is a rate determining step in the vaporization process.

V. STUDIES OF THE SUBLIMATION MECHANISM OF CADMIUM SULFIDE SINGLE CRYSTALS

Cadmium sulfide vaporizes according to the dominant reaction (Jeunehomme, 1962),

$$CdS(solid) \rightarrow Cd(vapor) + \frac{1}{2} S_2(vapor)$$

Crystals are available in high purity, crystallize in the wurtzite structure and show electronic conductivity. They are n-type (electrons are the majority charge carriers) under all conditions of stoichiometry. This is thought to be due to ionized sulfur vacancies, V_S^+, which predominate over ionized cadmium vacancies, V_{Cd}^- (Somorjai and Jepsen, 1964b; Woodbury, 1964). It has been found (Somorjai and Stemple, 1953) that the c-[(0001)]-face is stable under conditions of vacuum evaporation while the other low index face, the $(10\bar{1}0)$ or a-face, is not. The c-face remains invariant during the experiments, therefore, this face was used in most of the studies.

The temperature dependence (Somorjai, 1964; Somorjai and Jepsen, 1964a) of the vacuum evaporation rate of the (0001)-face of CdS has been measured in the temperature range 650-800°C. (Figure 6) The rates are more than an order of magnitude lower than the maximum evaporation rates calculated from equilibrium vapor pressure measurements (Somorjai, 1964; Neuhaus and Retting, 1958). The activation enthalpy and the heat of evaporation are $\Delta H^* = 50.3$ kcal and $\Delta H_v = 75.2$ kcal per mole of vaporizing solid, respectively.

A. Effect of Doping of CdS on its Evaporation Rate

1. Excess Cadmium and Sulfur in CdS

The free carrier concentration (electrons and holes) can be changed

by more than ten orders of magnitude by doping the CdS crystals with cadmium ($\sigma \sim 0.1$ mho cm^{-1}) or sulfur ($\sigma \sim 10^{-10}$ mho cm^{-1}) at elevated temperatures (900-1100°C) then quenching to freeze in the high temperature solubilities. Excess cadmium or sulfur in the crystals give rise to decreased initial evaporation rates. These crystals undergo a sharp transient and finally reach the steady state which is characteristic of undoped specimen. The conductivity change of the cadmium doped crystals indicates the out-diffusion of excess cadmium with a corresponding three to four orders of magnitude decrease in carrier concentration. The loss of excess cadmium is also indicated by the color change in the crystals. Cadmium doped samples are black to gray due to precipitated cadmium in the crystal lattice (Woodbury, 1964). Crystals, showing steady state evaporation rate, are yellow.

For cadmium- or sulfur doped CdS crystals the evaporation is controlled by the out-diffusion of excess cadmium or sulfur from the crystal lattice. As the excess surface cadmium evaporates it is replenished from the bulk by diffusion. As long as the diffusion rate of excess cadmium or sulfur is of the same order of magnitude or greater than the evaporation rate at a given temperature there is a constant "communication" between the bulk and the surface of the vaporizing crystal. Thus, bulk diffusion, which controls the surface concentration of excess cadmuim or sulfur, is the rate limiting step in this case.

If the diffusion rate of electrically active impurities is smaller than the evaporation rate, the impurity could not diffuse out of the crystal. Thus, there would be no transient evaporation, the constant impurity surface concentration would establish the evaporation rate

This is the case for copper impurity in CdS.

2. Effect of Copper-Doping of CdS

CdS single crystals can be uniformly doped by diffusing the surface evaporated copper into the crystal. When the CdS crystal is uniformly saturated with copper at the temperature of evaporation, the evaporation rate of Cu-doped CdS is decreased by more than 50 percent as shown in Fig. 7, over that of the evaporation rate of the undoped crystal (Somorjai and Lyon, 1965).

In order to investigate the dependence of CdS evaporation rate on the surface concentration of diffused copper, copper was vacuum deposited on only the $(000\bar{1})$-face of the undoped crystals. Then the (0001)-face was allowed to vaporize while copper diffuses into the crystal from the back surface (Somorjai and Lyon, 1965). This way the vaporizing surface retreats while the copper diffusion frontmoves toward the vaporizing face. As the copper profile reaches the vaporizing surface a rapid change in the copper surface concentration occurs which gives rise to an exponential decrease of the vaporization rate. When the copper surface concentration reaches its maximum, which corresponds to the solubility of copper in CdS at the evaporation temperature, a new lower steady state evaporation rate is established which is characteristic of the constant surface concentrations of copper ions.

B. The Effect of Light on the Evaporation Rate of CdS (Somorjai, 1964; Somorjai and Lester, 1965a)

The room temperature band gap of CdS is 2.41 eV and the temperature dependence of the gap is -5×10^{-4} eV/deg. Photons of energy greater than or equal to the band gap energy creates electron-hole pairs at the

vaporizing CdS surface, in excess of the equilibrium carrier concentration. If the vaporization is controlled by charge transfer an increase of the evaporation rate is expected in light with respect to the steady state rate in the dark, at a given temperature. For light to have an observable effect on the evaporation rate it is necessary that the electron-hole pair concentration produced by illumination should be of the same order of magnitude or larger than the free carrier concentration in the dark at the evaporation temperature (680-740°C). This criterion was met by using light intensities in the range 5.0×10^{3} - 2.0×10^{5} $\mu W/cm^{2}$. In addition, the trapping lifetime of photoelectrons and holes must be long enough, relative to the residence time of the neutral cadmium and/or sulfur species on the surface, to avoid direct electron-hole recombination prior to the desorption of the neutral species.

These conditions have been met for sulfur-doped CdS ($\sigma \sim 10^{-10}$ mho cm^{-1}). The effect of light on the evaporation rate of these crystals is shown in Fig. 8. The evaporation rate increases linearly with the light intensity in the studied range as shown in Fig. 9.

C. Surface Concentration Dependence of the Evaporation Rate CdS (Somorjai and Jepsen, 1964b)

The surface concentration of the final species of the reaction were varied using a molecular beam of sulfur and/or an atomic beam of cadmium (Somorjai and Jepsen, 1964a). Care was taken in all of the molecular beam experiments to maintain a sufficiently large mean free path of all vapor species in order to exclude possible gas phase interactions between the beam and species being evaporated from the CdS.

The molecules beams of S_2(vapor) or Cd(vapor) were prepared using

a double-oven arrangement which allowed preheating the impinging beam to that of the surface temperature of the vaporizing CdS crystal. The weight loss was monitored with a microbalance while the vapor flux was determined in separate measurements (Somorjai and Jepsen, 1964a). At low impingement rates, there is no observable effect. As the sulfur flux increases and becomes the same order of magnitude as that of the evaporation rate of CdS, the evaporation rate becomes proportional to the -1/2 power of the sulfur flux ($J_v \approx J_{S_2}^{-1/2}$).

Cadmium atomic beams had no appreciable effect on the evaporation rate of CdS in the range of impingement rates studies (Somorjai and Jepsen, 1964a).

From the results of the experiments we can now deduce the mechanism of CdS evaporation. The presence of excesses of cadmium, sulfur, and copper in CdS decreased the evaporation rates markedly. These impurities have low solubilities in cadmium sulfide, but they can change the free carrier concentration in the vaporizing crystals by orders of magnitude. It is apparent that the concentration of charge carriers plays an important role in the vaporization process. The effects of electrically active impurities and of light on the evaporation rate indicate that the vaporization is controlled by a charge transfer process. The vaporization reaction steps which can be deduced from the available experimental information are: a) diffusion of excess cadmium or sulfur to the surface, b) electron transfer to neutralize the cadmium ions at the surface, c) hole transfer to neutralize the sulfur ions at the surface, d) association of sulfur atoms, e) desorption of sulfur molecules, and f) desorption of cadmium atoms. Under vacuum evaporation conditions for undoped CdS

crystals in dark or in light, steps (b) and (c) are indistinguishable and rate limiting. For sulfur and cadmium doped crystals, reaction (a) controls the evaporation rate. For the vaporization of copper doped CdS, step (b) is the possible slow step.

VI. STUDIES OF THE SUBLIMATION MECHANISM OF GALLIUM ARSENIDE SINGLE CRYSTALS

Gallium arsenide has zinc blende structure and a melting point of 1238°C. It is a semiconductor* which is available in the highest purity.+ The compound vaporizes according to the dominant net reaction (Gutbier, 1961; Arthur, 1967)

$$GaAs(solid) \rightarrow Ga(vapor) + \frac{x}{2} As_2(vapor) + \frac{(1-x)}{4} As_4(vapor)$$

in the temperature range 750°-900°C. The tetramer arsenic concentration is about 25-65 mole % of the total arsenic flux and it is increasing with increasing temperature.

The vaporization characteristics of both, the (111) or gallium face and the $(\bar{1}\bar{1}\bar{1})$ or arsenic face were studied in this temperature range. These two low index faces should be composed dominantly of only one type of atoms and have been shown to have different oxidation (Miller, et al., 1961) and etching rates (Russell, et al., 1966; Gatos and Levine, 1960) under a variety of experimental conditions.

---

* The crystals which were used in the experiments were n-type, had room temperature resistivities of 0.1-0.2 ohm cm and mobility in the range 5×10^3 cm^2/volt sec).

\+ Purchased from Cominco American Inc., Spokane, Washington

A. Results

1. Microbalance Studies

The weight loss of the sample was measured as a function of time at a given temperature. From these data and the geometric surface area, the evaporation rate (mg/cm^2 -sec) was calculated. The surface area was not flat, of course, during the vaporization. The presence of small droplets of liquid gallium are readily discernible on both crystal faces (Lou and Somorjai, 1969). The area under the liquid is always smooth and deeper lying which indicates that a larger vaporization flux is emanating from the gallium coated area than from the uncoated portion of the surface.

A reproducible steady state vaporization rate could eventually be obtained at any temperature in the range of our study, regardless of the thermal history of the vaporizing crystal. There is however, always an induction period of transient evaporation at any given vaporization temperature before the steady state evaporation rate is obtained and this transient behavior very much depends on the thermal history. Figure 10 shows the vacuum evaporation rate of the gallium (111) and arsenic ($\bar{1}\bar{1}\bar{1}$) faces as a function of time at 800°C. The sample was (a) heated or (b) cooled to 800°C prior to the onset of the vaporization run. After heating to 800°C there is an initial induction period of slow vaporization after which the evaporation rate increases to attain the higher steady state rate. After cooling to 800°C there is a somewhat shorter initial induction period of rapid vaporization after which the evaporation rate decreases to attain the lower steady state rate. The observation that the steady state vacuum evaporation rate can be

established for the (111) and ($\bar{1}\bar{1}\bar{1}$) crystal faces indicate that both of these faces of gallium arsenide vaporize congruently even in the presence of liquid gallium on the vaporizing surfaces. The initial transient period during which the vaporization rate is changing is longer for the arsenic ($\bar{1}\bar{1}\bar{1}$) face than for the gallium (111) face.

The steady state vacuum evaporation rates were measured for both crystal faces of gallium arsenide as a function of temperature and are plotted in Fig. 11. The log R (mg/cm^{2}sec) vs. 1/T (°K) curves give straight lines above 750°C for both crystal faces which seem to overlap within the accuracy of the measurements. Here, we have also plotted the maximum evaporation rates obtained from equilibrium studies (Hove, 1955) as a function of temperature. These curves are parallel and their slopes give $E^* \simeq \Delta H_v^\circ = 90 \pm 4$ kcal/mole of solid. The vacuum evaporation rates however are less than one-third of the maximum rates in the temperature range 750°C-900°C. Thus, the average evaporation coefficient, $\bar{\alpha}(T)$ is about $\bar{\alpha}(T) \simeq 0.27$.

B. Mass Spectrometric Studies

During the vaporization of gallium arsenide the ions readily detectable in the mass spectra are As_4^+, As_2^+, As^+, and As_3^+. The dimer and tetramer ion peaks had the largest intensities and they were of comparable magnitude in the temperature range of our study. The experimental geometry (Fig. 2) has the advantage of allowing us to sample directly the vapor composition which emanates from the vaporizing gallium arsenide surface. Thus, any association reaction which may take place on the heater or chamber walls (Arthur, 1967) would only change

the background intensity distribution which can be measured independently and has been subtracted from the signal. Both the As^+ and As_2^+ can be identified (Lou and Somorjai, 1969) as fragmentation products of the electron impact ionization of As_2 and As_4 molecules.

The intensities of the As_2^+ and As_4^+ peaks which were detected during the vaporization of the gallium face (111) of gallium arsenide are plotted as a function of temperature in Fig. 12. The activation energies of vaporization are $E_D^* = 94.5$ kcal/mole and $E_T^* = 95.9$ kcal/mole of vapor respectively. The intensity ratios, As_2^+/As_4^+ which were obtained at different temperatures once steady state vaporization was reached are given in Table II. The log I^+T vs 1/T (°K) plots for the arsenic $(\bar{1}\bar{1}\bar{1})$ face are shown in Fig. 13. The activation energies of vaporization are $E_D^* = 99.6$ kcal/mole and $E_T^* = 142$ kcal/mole of vapor, respectively. The intensity ratios, As_2^+/As_4^+, which were obtained at different temperatures in steady state are also given in Table II. The results indicate that the activation energies of vaporization of tetramer arsenic molecules are markedly different for the two crystal faces. The activation energy for As_4 vaporization is larger for the arsenic $(\bar{1}\bar{1}\bar{1})$ face than for the gallium (111) face, $[E_T^*(\bar{1}\bar{1}\bar{1}) > E_T^*(111)]$ while for As_2, it is similar for both faces. This is clearly reflected in the tabulated intensity ratios.

C. Effect of Liquid Gallium on the Vaporization of GaAs

When the crystal faces were covered with excess liquid gallium and were then vaporized in vacuum the total evaporation rates (microbalance runs) increased more than three-fold and reached the maximum equilibrium value throughout the studied temperature range. Mass spectrometer studies also showed that the intensities of the As_2^+ and As_4^+ peaks increased markedly for both (111) and ($\bar{1}\bar{1}\bar{1}$) crystal faces with respect to the intensities detectable in the absence of liquid gallium. However, the intensity ratios, As_2^+/As_4^+, and the activation energies of vaporization for all of the arsenic species remained the same as that for the pure samples. Thus, the presence of liquid gallium on the vaporizing surface merely increases the evaporation rates of all of the vaporizing molecules. It does not change the vapor composition or the energetics of the vaporization surface reactions.

D. Discussion

The vacuum evaporation rates from both faces are roughly one-third of the maximum evaporation rate ($J^V(T)/J^V_{max}(T) = \bar{\alpha} = 0.28$) while the average activation energy of vaporization (kcal/mole of solid) is the same as the equilibrium heat of vaporization (kcal/mole of solid), $E^* \simeq \Delta H_V = 90 \pm 4$ kcal/mole of solid. The vaporization rate seems to be controlled by the magnitude of the pre-exponential factor of the overall rate equation $J(\text{mole/sec}) = K_0(S) \exp(-E^*/RT)$ where K_0 is a constant related to the frequency of attempted motion of a molecule over the energy barrier, E^*, and (S) is the concentration (moles/cm^2) of the molecules in the surface sites from which vaporization proceeds.

The vapor compositions (As_2/As_4) over the vaporizing (111) and ($\bar{1}\bar{1}\bar{1}$) faces of gallium arsenide were found to be different. This appears to be due to the markedly different activation energies of vaporization of the tetramer (As_4) molecules from the gallium ($E^* = 95.9$ kcal/mole of vapor) and the arsenic ($E^* = 142$ kcal/mole of vapor) crystal faces, respectively. This result indicates that the formation of the tetramer molecules is dependent on some physical-chemical or structural property of the particular crystal face. Differences in dislocation densities (Lester and Somorjai, 1968), charge density distributions (Somorjai and Lester, 1967), or impurity concentrations (Somorjai and Lester, 1967) in the (111) and ($\bar{1}\bar{1}\bar{1}$) faces may play an important role in determining the surface concentration of the vaporizing species.

In the presence of liquid gallium the total vaporization rate increases to obtain the maximum equilibrium rate. At the same time, however, the vapor compositions on both faces remain unaffected by the presence of the liquid metal. It appears that liquid gallium merely increases the number of surface sites from which vaporization can proceed. It does not change the mechanism of vaporization which would be reflected in the lowering of the activation energy of vaporization or in the changing of the vapor composition. Thus, Ga(l) does not shift the equilibrium in any way between gallium and arsenic species on the gallium arsenide surface. There is evidence from other vaporization studies that different liquid metals of low vapor pressure (In and Ga on GaN [Schoonmaker, et al., 1965], Tl on As [Brewer and Kane, 1955]) can also accelerate the evaporation of IIIA-VA or VA compounds. Therefore, liquid gallium may not be the only liquid metal which can increase the evaporation rate of gallium

arsenide; other metals most likely could also speed up the evaporation process.

Several observations indicate that there is no equilibrium between the dimer (As_2) and tetramer (As_4) arsenic molecules on the vaporizing surface. If the tetramers were formed via the equilibrium association of dimers, $2D \leftrightharpoons T$ (an exothermic reaction [Arthur, 1967] $\Delta H = -62$ kcal/mole), then the dimer to tetramer ratio, As_2/As_4, would have decreased while the evaporation rate increases in the presence of liquid gallium $D/T \approx 1/D$. This does not happen. The presence of the liquid metal does not change the vapor compositions on the two studied surfaces. In addition, the experimental fact that the dimer to tetramer ratios are different on the two crystal faces indicate that equilibrium between these molecules cannot be established at least on one of the crystal faces.

We find from microbalance studies that the average activation energies of vaporization and the total sublimation rates are identical for the two [(111) and ($\bar{1}\bar{1}\bar{1}$)] crystal faces in the temperature range of our study. Mass spectrometric studies indicate however, that the activation energy of vaporization of the tetramer arsenic molecules is markedly different for the two crystal faces. If the sublimation of gallium arsenide is congruent the sum of the activation energies of vaporization of all vaporizing species has to be the same for both faces. Thus, it is likely that the activation energy of sublimation of gallium may also be different for the (111) and ($\bar{1}\bar{1}\bar{1}$) orientations of gallium arsenide. Studies to ascertain this effect are in progress.

VII. LOW ENERGY ELECTRON DIFFRACTION (LEED) STUDY OF THE VAPORIZING SILVER (100) SURFACE

The diffraction of low energy electrons (5-500 eV) from single crystal surfaces can be used to obtain information about the structure of surfaces on an atomic scale (Somorjai, 1968b). The diffraction pattern is representative of the periodic arrangements of atoms in the surface. In these experiments a monochromatic electron beam is back-scattered from one face of a single crystal and the elastically scattered fraction of electrons post-accelerated onto a fluorescent screen where the diffraction pattern is displayed. The studies have to be carried out in ultra high vacuum ($< 10^{-8}$ torr) to avoid possible contamination of the sample surface by the adsorption of gases from the ambient (Morabito, et al., 1968; Somorjai, 1968b).

One important discovery of low energy electron diffraction studies in recent years is that surface atoms may reside in different kinds of surface structures (Somorjai, 1968b). The presence of these structures is indicated by the appearance of extra diffraction features in the LEED pattern which are superimposed on the diffraction pattern of the surface unit mesh which is predicted by the bulk unit cell. The surface structures can be characterized by lattice parameters which are integral multiples of the unit cell dimensions which characterize the bulk unit cell. Most semiconductors (Si, Ge, GaAs, CdS) and insulators (Al_2O_3) which have been studied so far, exhibit surface rearrangements (Somorjai, 1968b). Among the metals only Au, Pt, Bi and Sb were found to rearrange while Al or Ni have surface unit mesh which are expected from their bulk unit cell (Somorjai, 1968b).

The purpose of these continuing studies is to obtain information about the atomic structure of the vaporizing surface. We would like to determine whether vaporization occurs from an ordered surface where most atoms occupy equilibrium lattice sites or whether vaporization takes place from a liquid-like surface layer in which long range order, which is characteristic of the bulk crystal, has been destroyed. LEED should be sensitive to detect and monitor changes in the surface structure.

It is well known (Somorjai and Lester, 1967; Lester and Somorjai, 1968) that the surface which vaporizes into vacuum becomes "rough", i.e. exhibits high density of steps, pits and ledges. These macroscopic changes in the surface structure cannot, in general, be detected by low energy electron diffraction. The lateral coherence length of low energy electrons is of the order of $\sim 10^2$ Å. As long as the distance between steps is larger than the coherence length the conditions for constructive interference between the scattered electrons is not affected. Thus, the presence of steps in the surface would not alter the diffracted electron beam intensities.

If the step or defect densities in the surface become so high that the ordered domains are reduced in size below $(\sim 10^2)^2$ Å^2, the intensity of the diffraction features decreases markedly, i.e., LEED becomes sensitive to surface roughness. Figures 14a and 14b show diffraction patterns of the (100) face of platinum, a) before ion bombardment (by 300 eV argon ions) and b) after ion bombardment. As a result of ion bombardment damage the spots become less intense and large. It should be noted that the spot width is proportional to 1/N where N is the number of atoms in the ordered domains.

Ordered arrangements of surface defects or steps could, of course, also be detectable by low energy electron diffraction. Recently, the presence of ordered rows of steps in the ( ) face of uranium dioxide has been reported by Ellis.

Silver is a face centered cubic metal, it has a melting point of 961°C. The metal has a high vapor pressure at the melting point ($> 10^{-3}$ torr) and its vapor is composed primarily of monatomic gaseous species. Vacuum sublimation studies (Winterbottom and Hirth, 1964) indicate that, after a short induction period, the maximum sublimation rate is obtained within the accuracy of the experiments. The activation energy of sublimation is equal to the heat of sublimation ($E^* \simeq \Delta H_v$). It appears that equilibrium can be established in all the surface reaction steps which lead to vaporization and that the desorption of silver atoms from the vaporizing surface requires no activation energy.

The (100) crystal face of silver was vaporized in a low energy electron diffraction chamber under conditions of free vaporization in the temperature range of 600-930°C. The diffraction pattern was detected and monitored during vaporization. The sample was then quenched to room temperature and the intensities of the diffraction spots were recorded. It should be noted that the intensity of the diffracted beams decreases exponentially with increasing temperature of the solid. This well-known effect (Debye-Waller effect) is due to the increased mean displacement of surface atoms with increasing temperature (Somorjai, 1968b).

The results of this low energy electron diffraction study indicate that the vaporizing Ag(100) surface retains its structure and long range

order. No significant changes in either the arrangement or the intensity of the diffraction spots were found to occur during vaporization. Thus, it appears that the vaporizing silver surface is ordered and certainly not liquid-like as far as it can be determined by the LEED technique.

VIII. CONCLUSIONS

The sublimation mechanisms of sodium chloride, cadmium sulfide and gallium arsenide simple crystals have been studied in considerable detail. Although the experimental information is insufficient to develop a more general theory of vaporization we can identify several important parameters which seem to control the sublimation rate of different groups of compounds.

A. Composition of the Surface

Minute deviations from the solid state composition (excess vacancies) which produced a steady state sublimation rate have markedly changed the evaporation rate. Changes in the surface concentration of gallium in GaAs, cadmium or sulfur in CdS give rise to transient evaporation rates which approach the steady state value only slowly. It is likely that the marked lowering of the sublimation rates of calcium-doped NaCl may also be due to changes in the composition of the surface. The presence of divalent ions in the alkali halide crystal lattice creates a large concentration of sodium ion vacancies in excess of their steady state concentration in the pure crystals. In addition to point defects, line defects such as dislocations could also markedly influence the sublimation rate (NaCl). This effect should be detectable in solids where there is a low mobility of dislocations so that they cannot anneal out at the sublimation temperatures.

B. Charge Transfer

It is apparent that the capture of mobile charge carriers (electrons and holes) by the cadmium and sulfur ions to form neutral species which may vaporize is a rate controlling step in the vaporization of CdS. Charge

transfer may also play an important role in the sublimation of gallium arsenide although conclusive experimental evidence is lacking at the present. The effect of liquid metals which accelerate the sublimation process of IIIA-VA compounds may be through their providing a source of free electrons which facilitates both, the dissociation of the crystal and the association of the vaporizing species (As_2, As_4). In alkali halides where the electrons are tightly held and sublimation occurs by ion pairs charge transfer may not be expected to be an important reaction step.

C. Impurities

Impurities which are electrically active (copper in CdS) or change the solid composition (calcium in NaCl) can markedly change the sublimation rates. It is likely that similar effects will be found in GaAs as well.

There are several observations which seem to hold for all three groups of compounds which we have investigated.

D. Concurrent Vaporization Mechanisms

For NaCl and GaAs the vapor fluxes are composed of more than one type of vapor molecules. There seems to be no equilibrium on the vaporizing surface between NaCl and Na_2Cl_2 or As_2 and As_4 molecules. Sublimation occurs by two indepedent reaction paths under all conditions which we have investigated. Surface diffusion which would allow reaction between the molecules does not seem to take place in these surfaces.

E. Invariance of Vapor Composition

We have studied all three compounds under a variety of experimental conditions which have changed their evaporation rates by one to two orders of magnitude. The steady state vapor compositions however remained virtually unchanged within the accuracy of the experiments under all conditions of sublimation.

Acknowledgement - This work was performed under the auspices of the United States Atomic Energy Commission.

REFERENCES

Arthur, J. R. (1967). J. Phys. Chem. Solids 28, 2257.

Berkowitz, J., and Chupka, W. A. (1958). J. Chem. Phys. 29, 653.

Brewer, L. and Kane, J. S. (1955). J. Phys. Chem. 59, 105.

Burton, W. K., Cabrera, N. and Frank, F. C. (1951). Phys. Trans. Roy. Soc. (London) A243, 299.

Gatos, H. C. , and Levine, M. C. (1960). J. Electrochem. Soc. 107, 427.

Gutbier, H. B. (1961). Z. Naturforsch. 16a, 268.

Hertz, H. (1882). Ann. Phys. (Leipzig) 17, 177.

Hove, J. E. (1955). Phys. Rev. 99, 480.

Jeunehomme, M. (1962). Ph.D. Dissertation, University Libre de Bruxelles, Belgium.

Kane, J. S. (1955). Ph.D. Dissertation, University of California, Berkeley.

Knudsen, M. (1915). Ann. Phys. (Leipzig) 47, 697.

Langmuir, I. (1913). J. Am. Chem. Soc. 35, 931.

Lester, J. E., and Somorjai, G. A. (1968). J. Chem. Phys. 49, 2940.

Lou, K., and Somorjai, G. A. (1969). J. Phys. Chem. (to be published).

Melville, H. (1936). Trans. Faraday Soc. 32, 1017.

Miller, D. P., Harper, J. G., and Perry, T. R. (1961). J. Electrochem. Soc. 108, 1123.

Morabito, J. M., and Somorjai, G. A. (1968). J. Metals, 20, 17.

Morabito, J. M., Steiger, R. F., Muller, R. H., and Somorjai, G. A. (1969). Proc. Fourth International Materials Symposium, University of California, Berkeley, June 19-21 (1968). To be published by J. Wiley and Sons, Inc.

Neuhaus, A., and Retting, W. (1958). Z. Electrochemie, 62, 33.

Palmberg, P. W., and T. N. Rhodin. (1968). J. Appl. Phys. 39, 2425.

Rosenblatt, G. (1963). J. Electrochem. Soc. 110, 563.

Rosenblatt, G. M., and Lee, Pang-Kai. (1968). J. Chem. Phys. 49, 2995.

Russell, G. J., Lip, H. K., and Haneman, D. (1966). J. Appl. Phys. 3328.

Schoonmaker, R. C., Buhl, A., and Lemley, J. (1965). J. Phys. Chem. 69, 3455.

Searcy, A. W. (1968). Pacific Conference on Chemistry and Spectroscopy. San Francisco, California, November 6-8.

Somorjai, G. A. (1964a). In "Condensation and Evaporation of Solids" (E. Rutner, P. Goldfinger and J. P. Hirth, eds.), Gordon and Breach Science Publishers, New York.

Somorjai, G. A. (1964b). Surface Sci. 2, 298.

Somorjai, G. A. (1968a). Science, 162, 755.

Somorjai, G. A. (1968b). Ann. Rev. Phys. Chem. 19, 251.

Somorjai, G. A., and Jepsen, D. W. (1964a). J. Chem. Phys. 41, 1389.

Somorjai, G. A., and Jepsen, D. W. (1964b). J. Chem. Phys. 41, 1394.

Somorjai, G. A., and Lester, J. E. (1965a). J. Chem. Phys. 42, 4140.

Somorjai, G. A., and Lester, J. E. (1965b). J. Chem. Phys. 43, 1450.

Somorjai, G. A., and Lester, J. E. (1967). Prog. in Solid State Chem. 4, 1.

Somorjai, G. A., and Lyon, H. B. (1965). J. Chem. Phys. 43, 1456.

Somorjai, G. A., and Stemple, N. R. (1953). J. Appl. Phys. 35, 3398.

Stranski, I. N. (1928). Z. Phys. Chem. 136, 259.

Winterbottom, W. L., and Hirth, J. P. (1964). In "Condensation and Evaporation of Solids" (E. Rutner, P. Goldfinger, and J. P. Hirth, eds.) Gordon and Breach Science Publishers, New York.

Winterbottom, W. L. (1966). Ph.D. Dissertation, Carnegie Institute of Technology.

Woodbury, H. H. (1964). Phys. Rev. 134, 492.

Ziman, B., and Moyer, J. (1944). J. Chem. Phys. 12, 362.

Table I - Activation energies of vaporization for NaCl crystals with different dislocation densities

Dislocation Density	$.8 \times 10^6/cm^2$	$1 \times 10^8/cm^2$	$2 \times 10^6/cm^2$	$\sim 4 \times 10^6/cm^2$	$\sim 6 \times 10^6$	$>15 \times 10^6/cm^2$
E_M^* (kcal/mole)	50.7 ± 1	52.4 ± 1.5	54.0 ± 1	55.6 ± .6	53.8 ± 1.1	56.6 ± 1.1
E_D^* (kcal/mole)	58.2 ± 1	61.5 ± 1.6	62.0 ± 4	65.6 ± .6	63.3 ± .8	62.8 ± .9

Table II. The intensity ratios, As_2^+/As_4^+, for the gallium (111) and arsenic ($\bar{1}\bar{1}\bar{1}$) faces at different temperatures.

Ga(111) face		As($\bar{1}\bar{1}\bar{1}$) face	
T (°C)	As_2^+/As_4^+	T (°C)	As_2^+/As_4^+
728	0.47	705	3.57*
730	0.48	746	0.81
758	0.44	798	0.78
780	0.49	809	0.73
782	0.51	842	0.71
832	0.44		
838	0.48		

* May not have reached steady state

FIGURE CAPTIONS

Fig. 1 Scheme of the experimental arrangement used in the microbalance studies of the total vaporization rate.

Fig. 2 Scheme of the mass spectrometer system.

Fig. 3 Evaporation rate of low and high dislocation density sodium chloride single crystals as a function of temperature. Etch pit densities, O - 1×10^{6} cm^{-2}; Δ - 1×10^{7} cm^{-2}. Equilibrium data from Zimm and Meyer (1944).

Fig. 4 Representative curves of the ion intensities, Na^{+}(□), $NaCl^{+}$ (O) and Na_2Cl^{+} (■) and the monomer to dimer ratio, M/D, as a function of temperature.

Fig. 5 Evaporation rates of calcium-doped sodium chloride crystals (●) and of pure crystals with different dislocation densities.

Fig. 6 Rate of evaporation of CdS single crystal c-face as a function of reciprocal temperature.

Fig. 7 Evaporation rate of the (0001)-face of CdS at 700°C . The crystal was copper doped at 700°C. Dotted line shows the evaporation rate of undoped crystal.

Fig. 8 The evaporation rate of sulfur-doped (1200°C, 20 atm) CdS single crystal c-face, X - in dark; and ● - in light at 696°C.

Fig. 9 Light intensity dependence of the evaporation rate of sulfur-doped (1200°C, 20 atm) CdS single crystal c-face at 696°C. 100 percent = 2.0×10^{5} $\mu W/cm^{2}$.

Fig. 10 The evaporation rates of the (111) and ($\bar{1}\bar{1}\bar{1}$) faces of gallium arsenide as a function of time at T = 750°C.

Fig. 11 The evaporation rates of the (111) and ($\bar{1}\bar{1}\bar{1}$) faces of gallium arsenide as a function of temperature. Equilibrium data from Arthur (19).

Fig. 12 Representative curves of the ion intensities, As_2^+ and As_4^+ as a function of temperature for the (111) face of GaAs.

Fig. 13 Representative curves of the ion intensities, As_2^+ and As_4^+ as a function of temperature for the ($\bar{1}\bar{1}\bar{1}$) face of GaAs.

Fig. 14 a) Diffraction pattern of an annealed face centered cubic metal (100) face at E = 58 eV; b) pattern after ion bombardment.

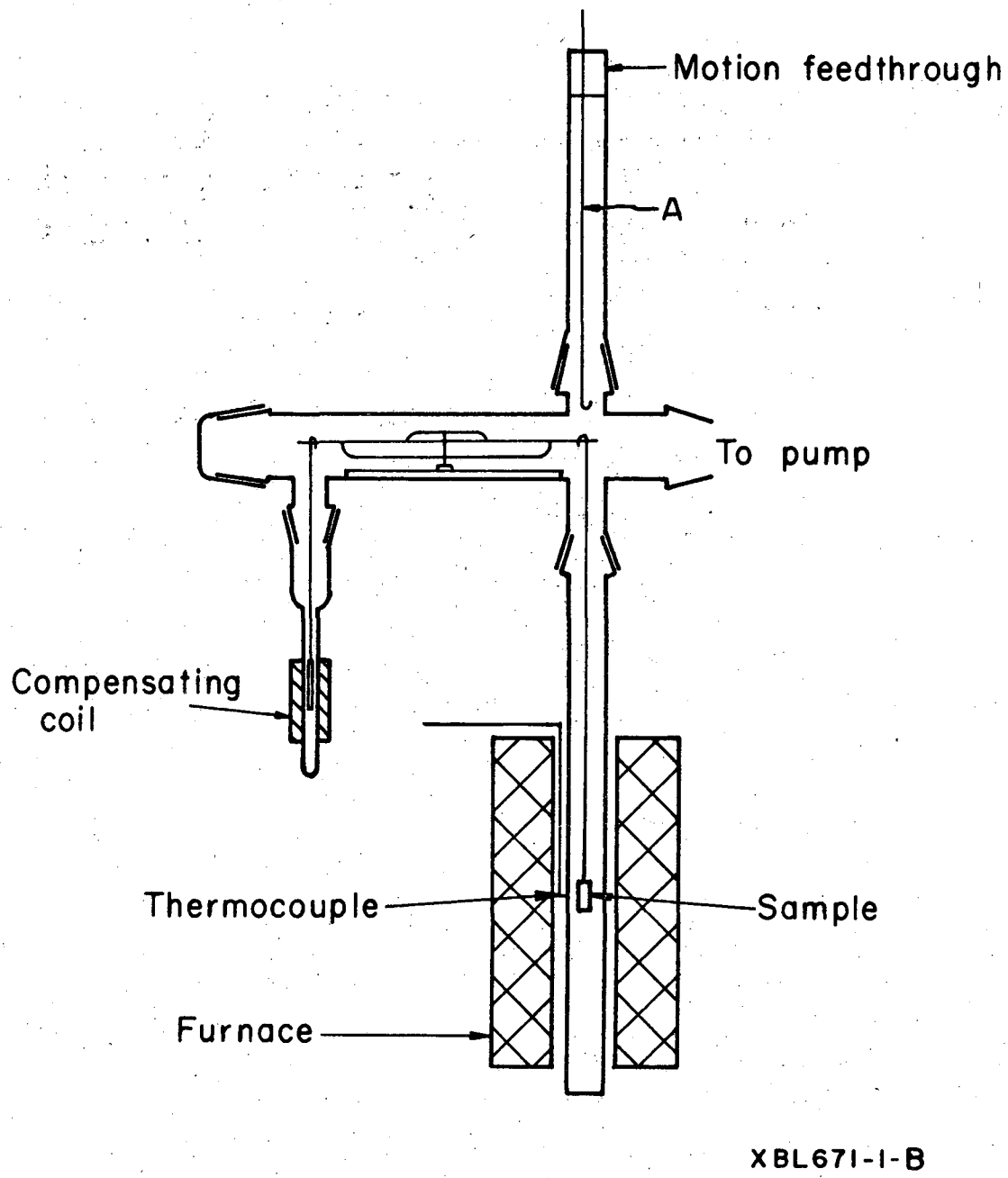
Motion feedthrough
A
To pump
Compensating coil
Thermocouple
Sample
Furnace
XBL671-1-B

Fig. 1

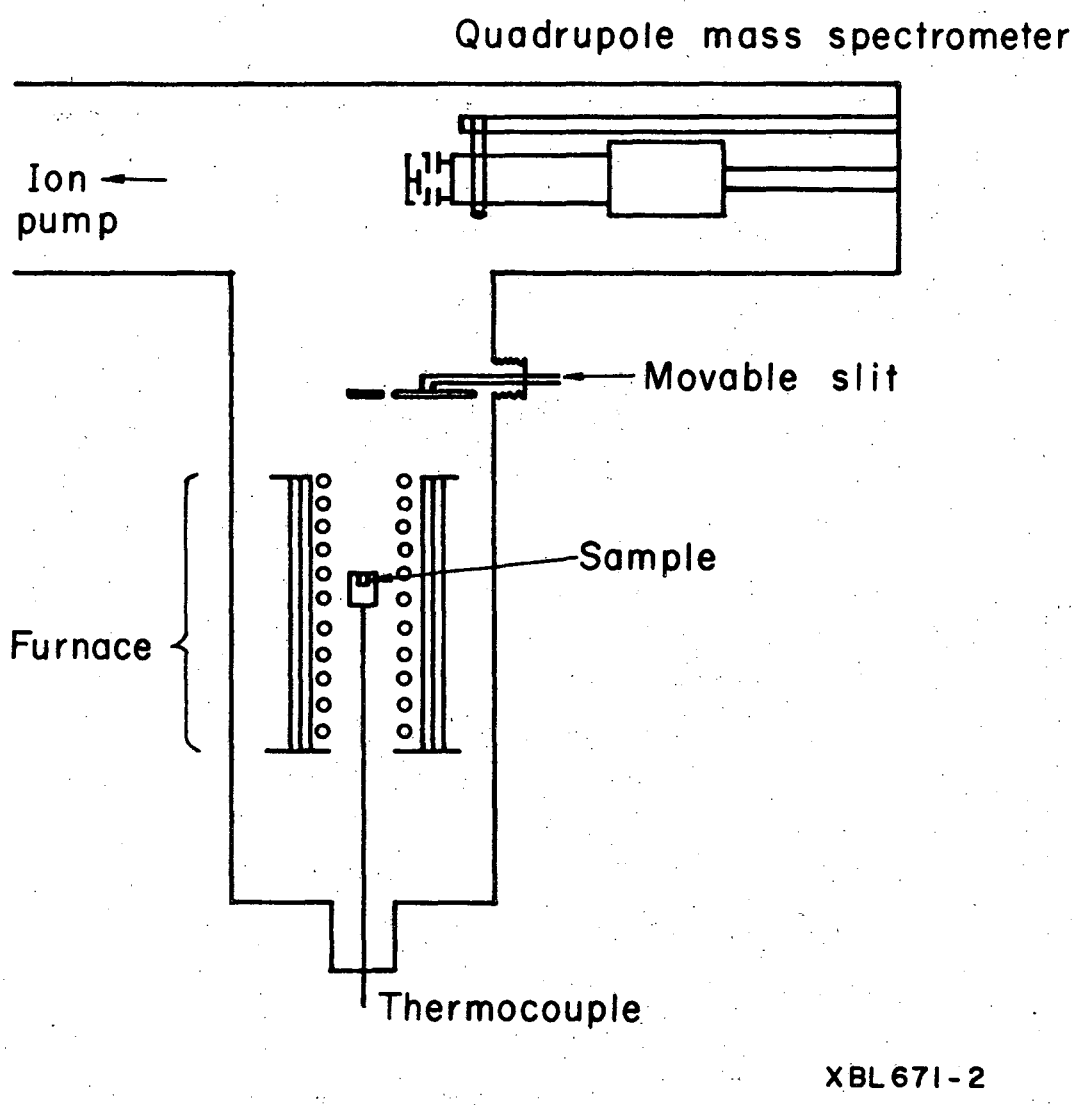
Quadrupole mass spectrometer
Ion pump
Movable slit
Sample
Furnace
Thermocouple
XBL671-2

Fig. 2

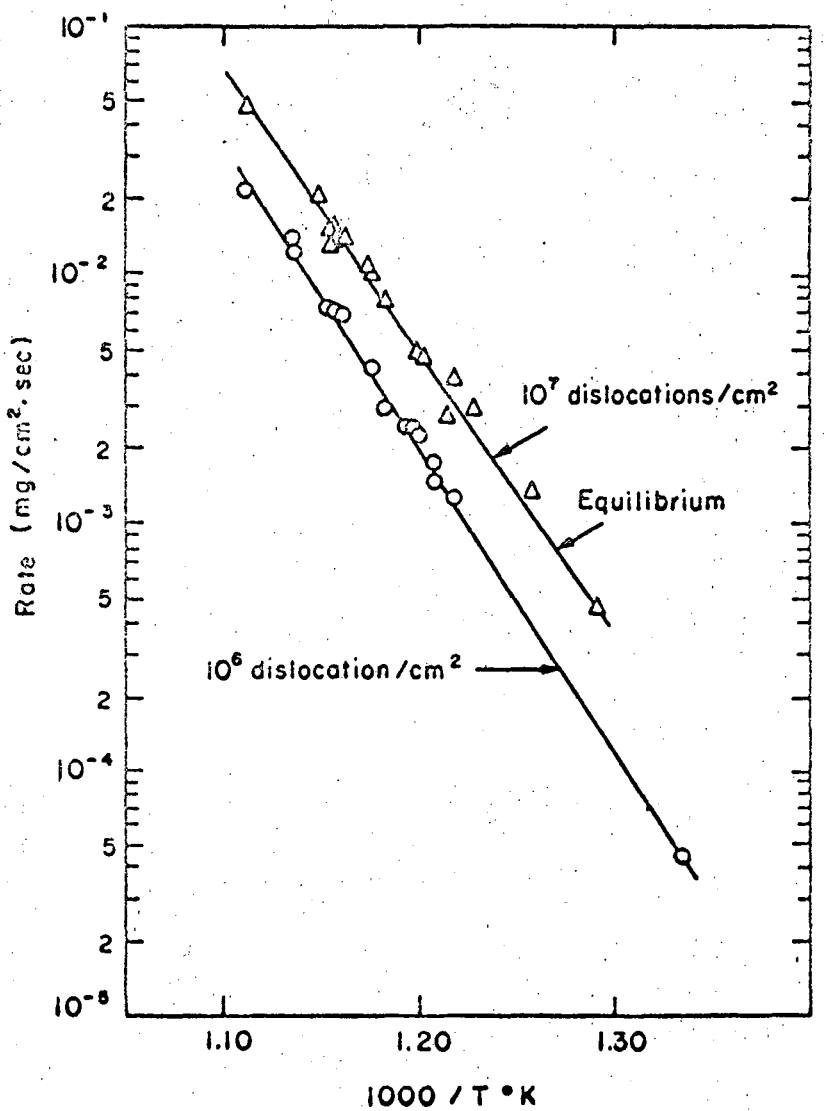
Rate (mg/cm²·sec)
10⁻¹
5
2
10⁻²
5
2
10⁻³
5
2
10⁻⁴
5
2
10⁻⁵
1.10
1.20
1.30
1000 / T °K
10⁷ dislocations/cm²
Equilibrium
10⁶ dislocation/cm²

Fig. 3

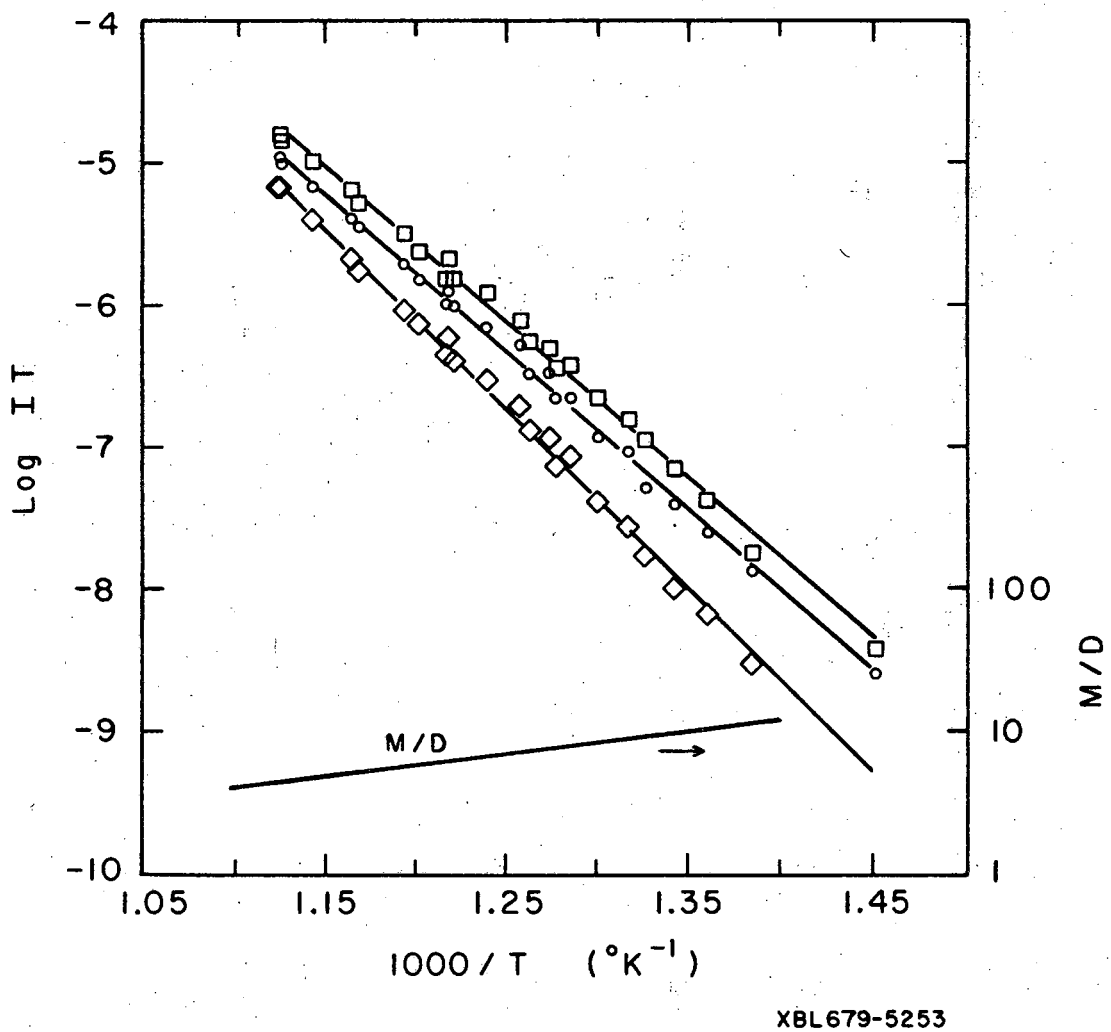
-4
-5
-6
-7
-8
-9
-10
Log I T
100
10
1
M/D
M/D
1.05
1.15
1.25
1.35
1.45
1000 / T (°K⁻¹)
XBL679-5253

Fig. 4

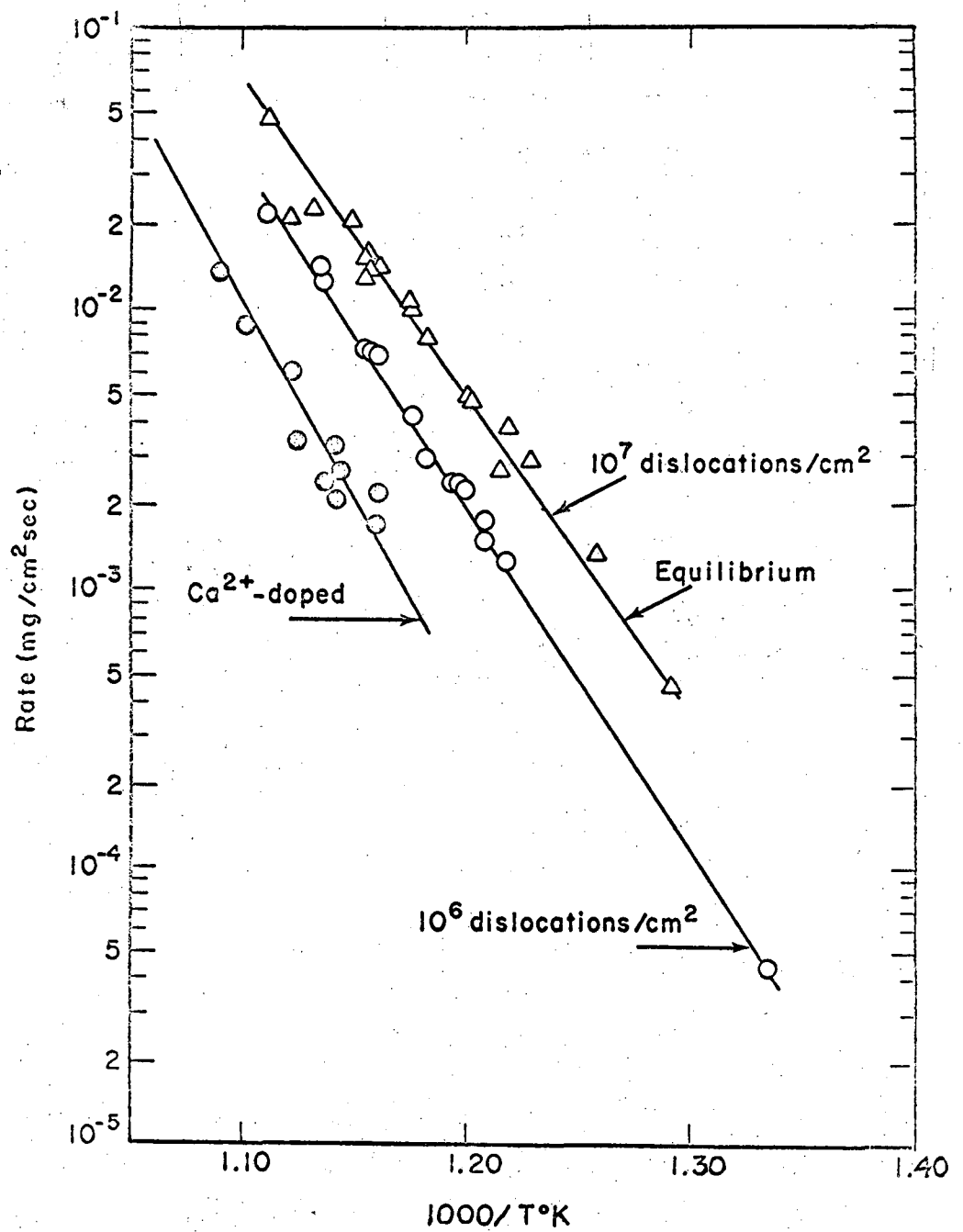

XBL 6812-6289

Fig. 5

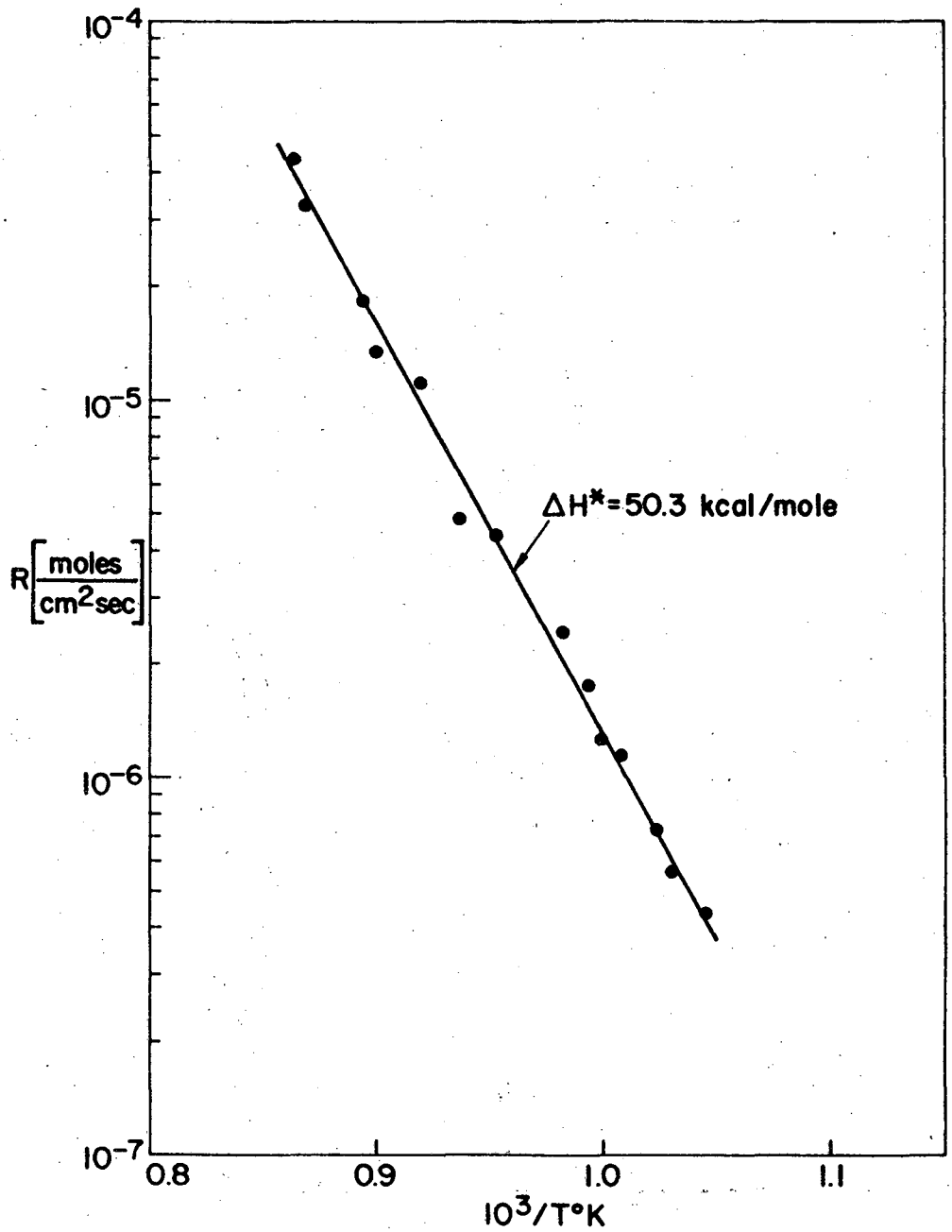

MUB-11015

Fig. 6

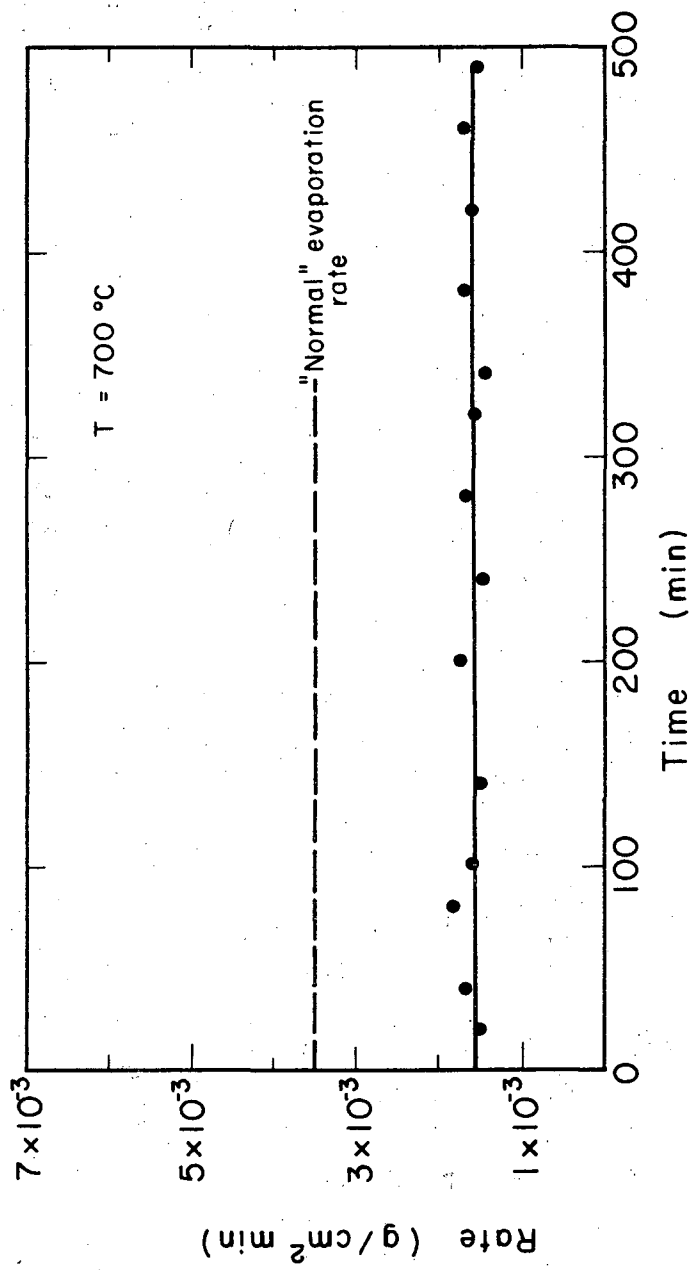

MUB-5954

Fig. 7

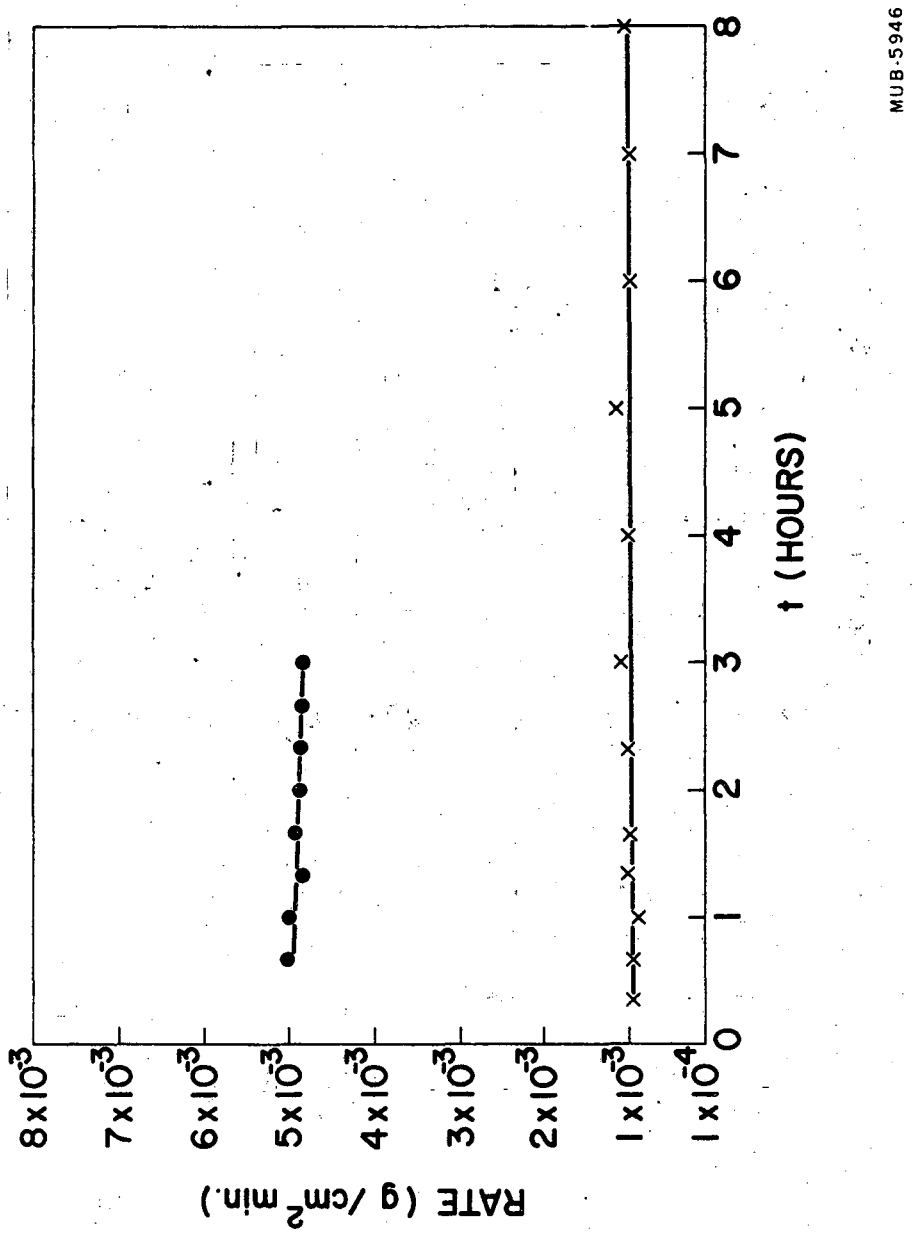
RATE (g /cm^2 min.)
8x10^{-3}
7x10^{-3}
6x10^{-3}
5x10^{-3}
4x10^{-3}
3x10^{-3}
2x10^{-3}
1x10^{-3}
1x10^{-4}
0
1
2
3
4
5
6
7
8
t (HOURS)
MUB-5946

Fig. 8

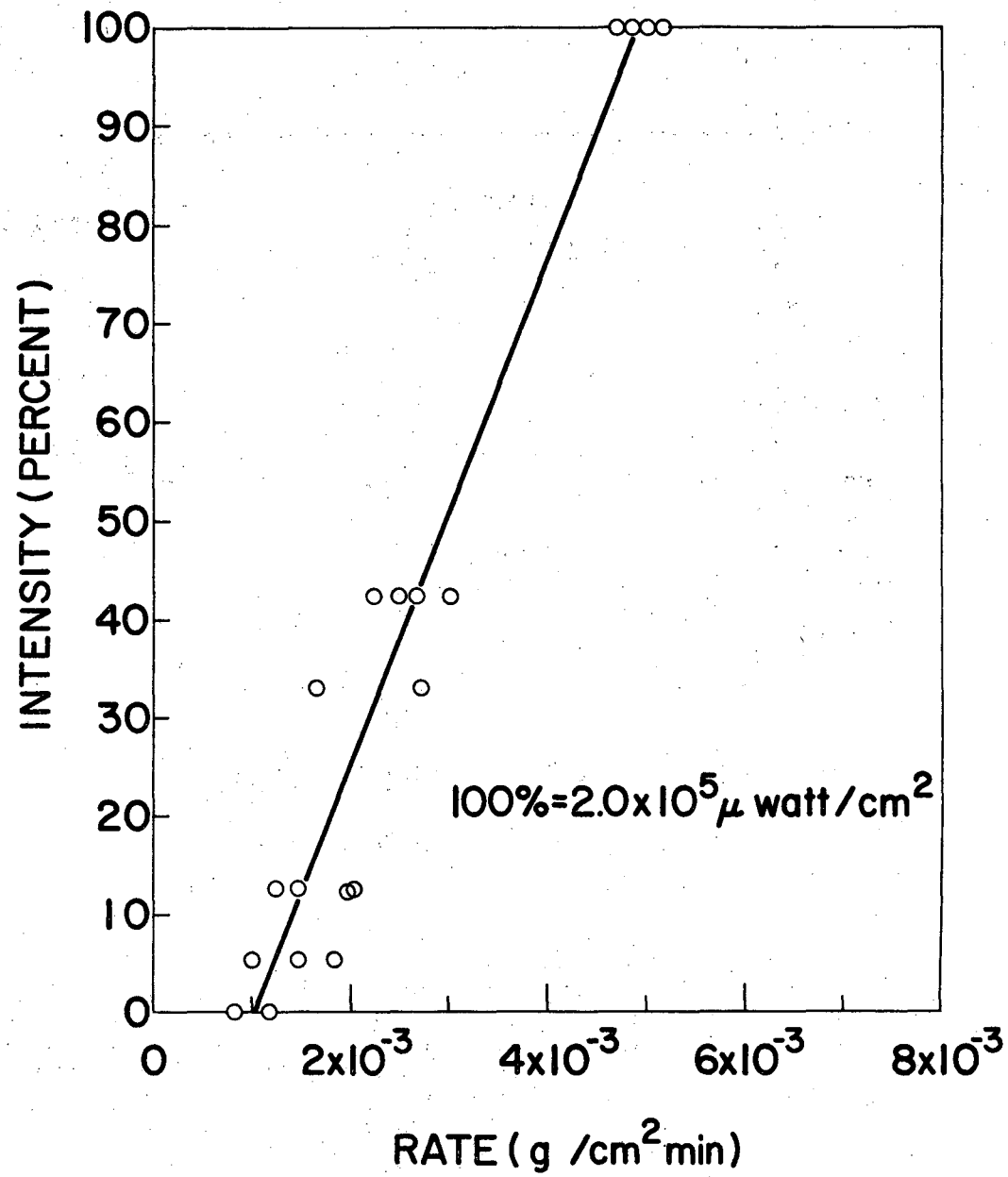

MUB-5947

Fig. 9

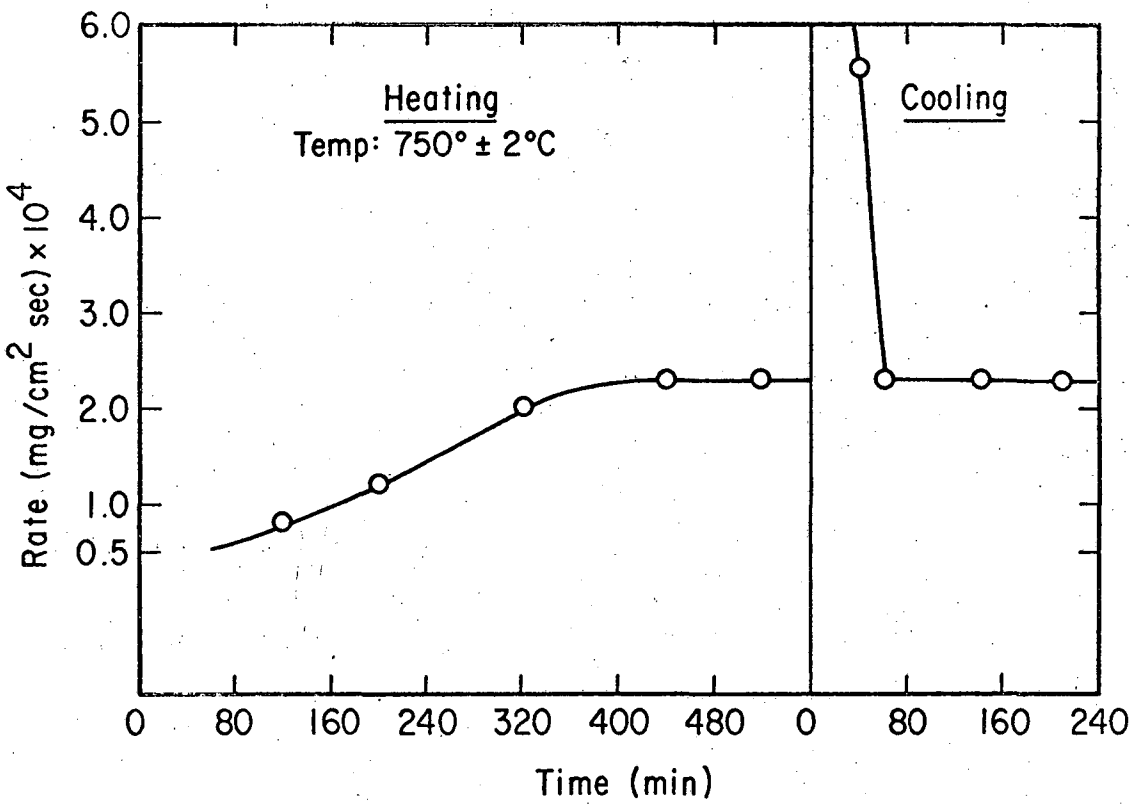

XBL 6812-6290

Fig. 10

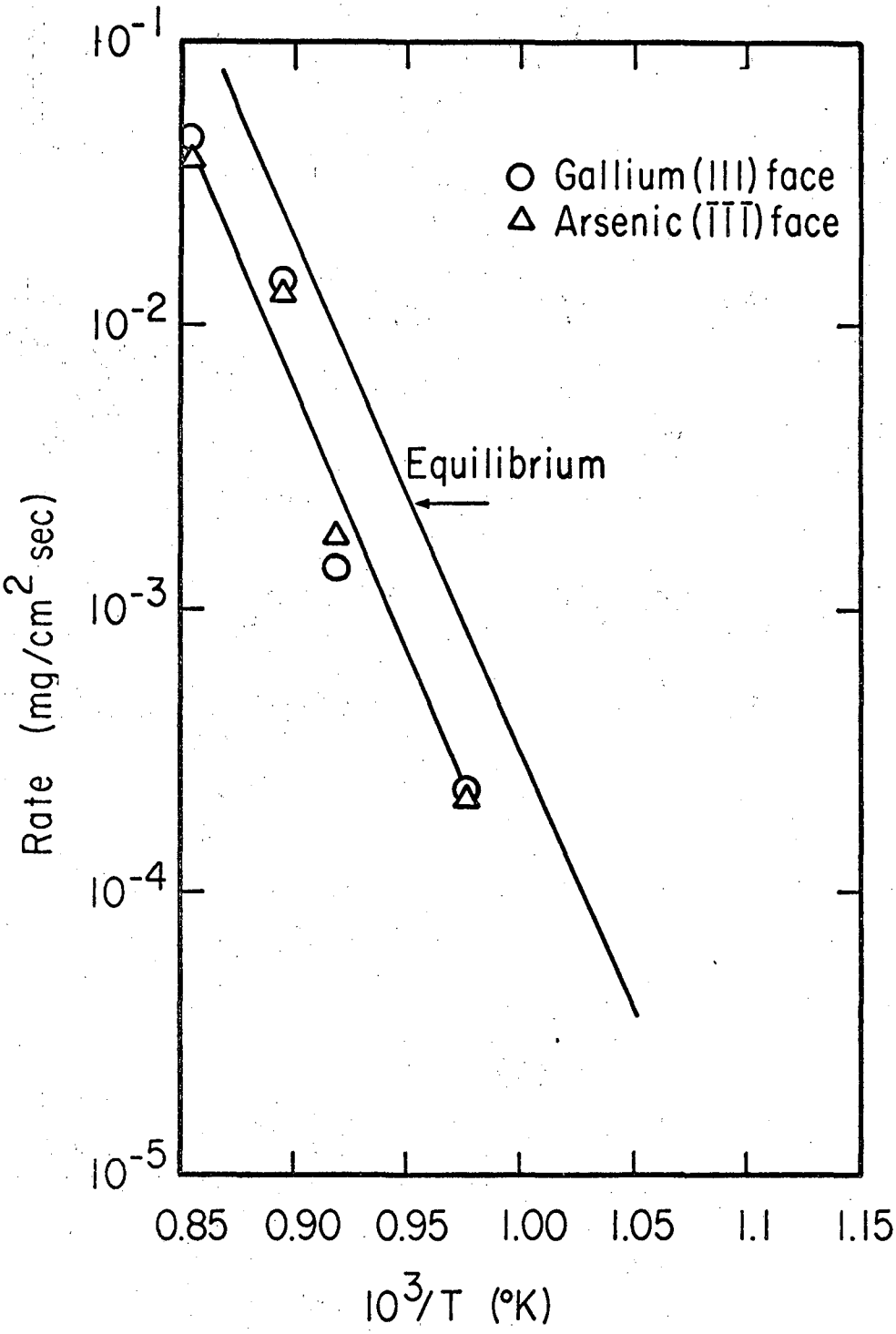

XBL 6812-6291

Fig. 11

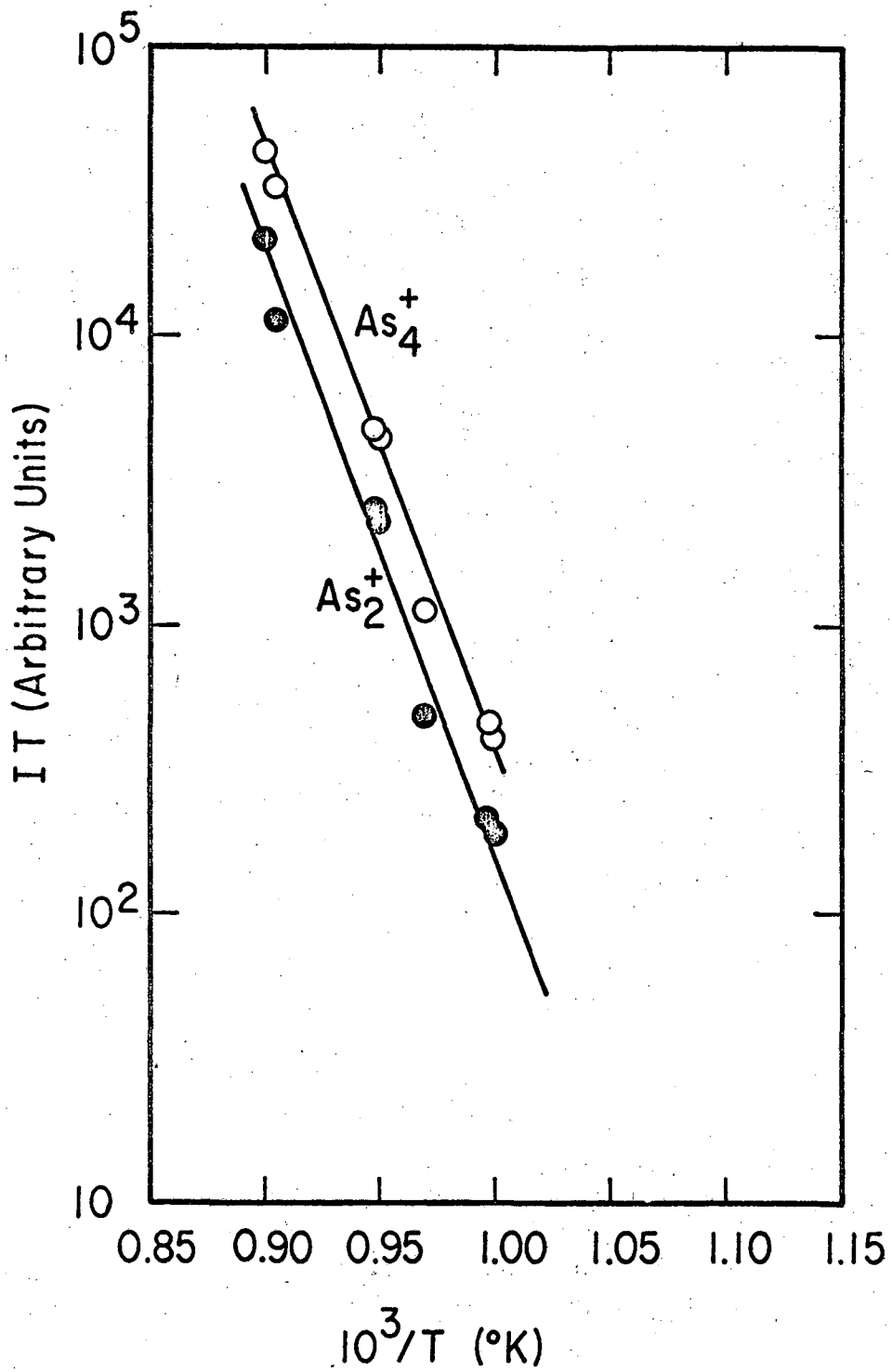

XBL 6812-6292

Fig. 12

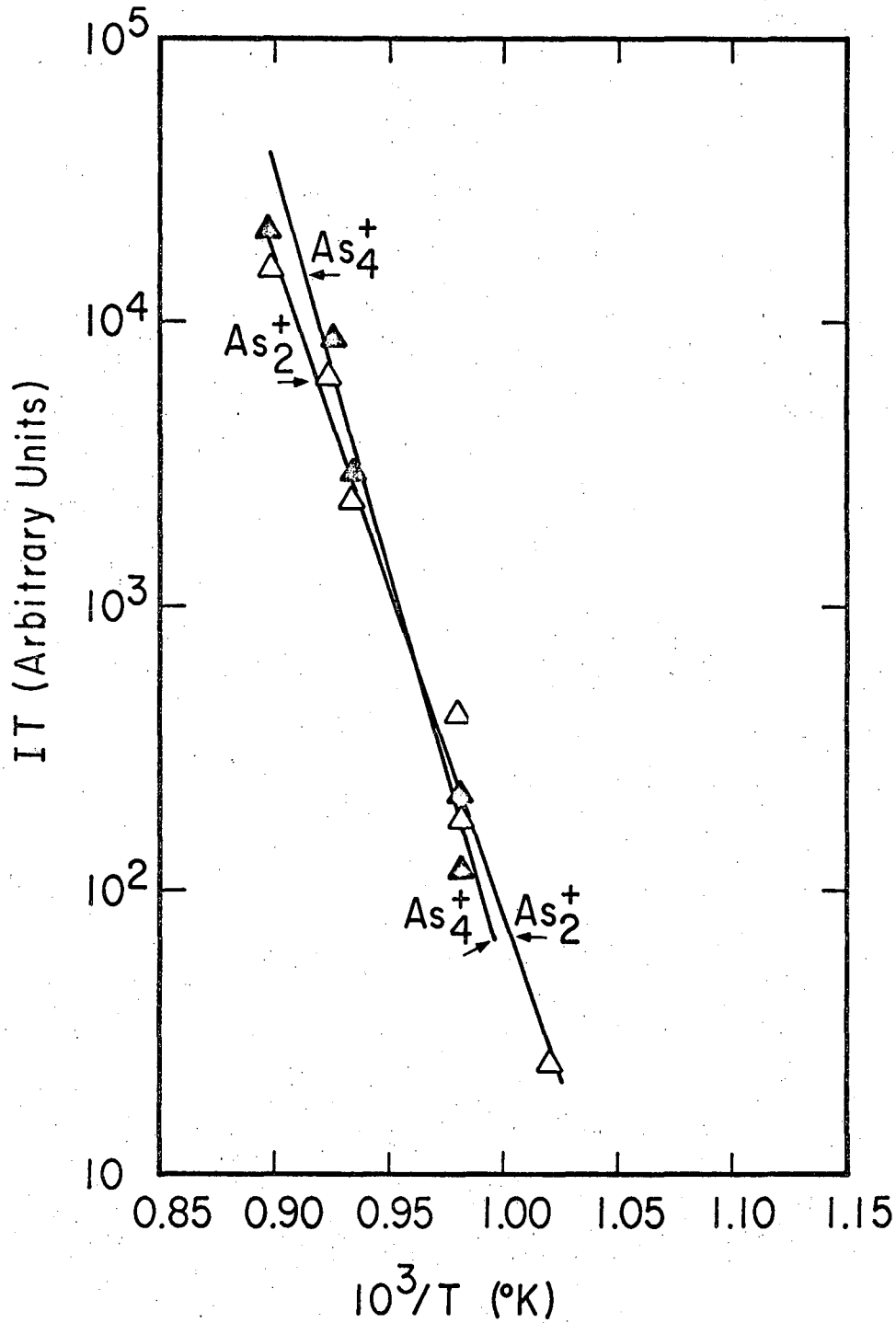

XBL 6812-6293

Fig. 13

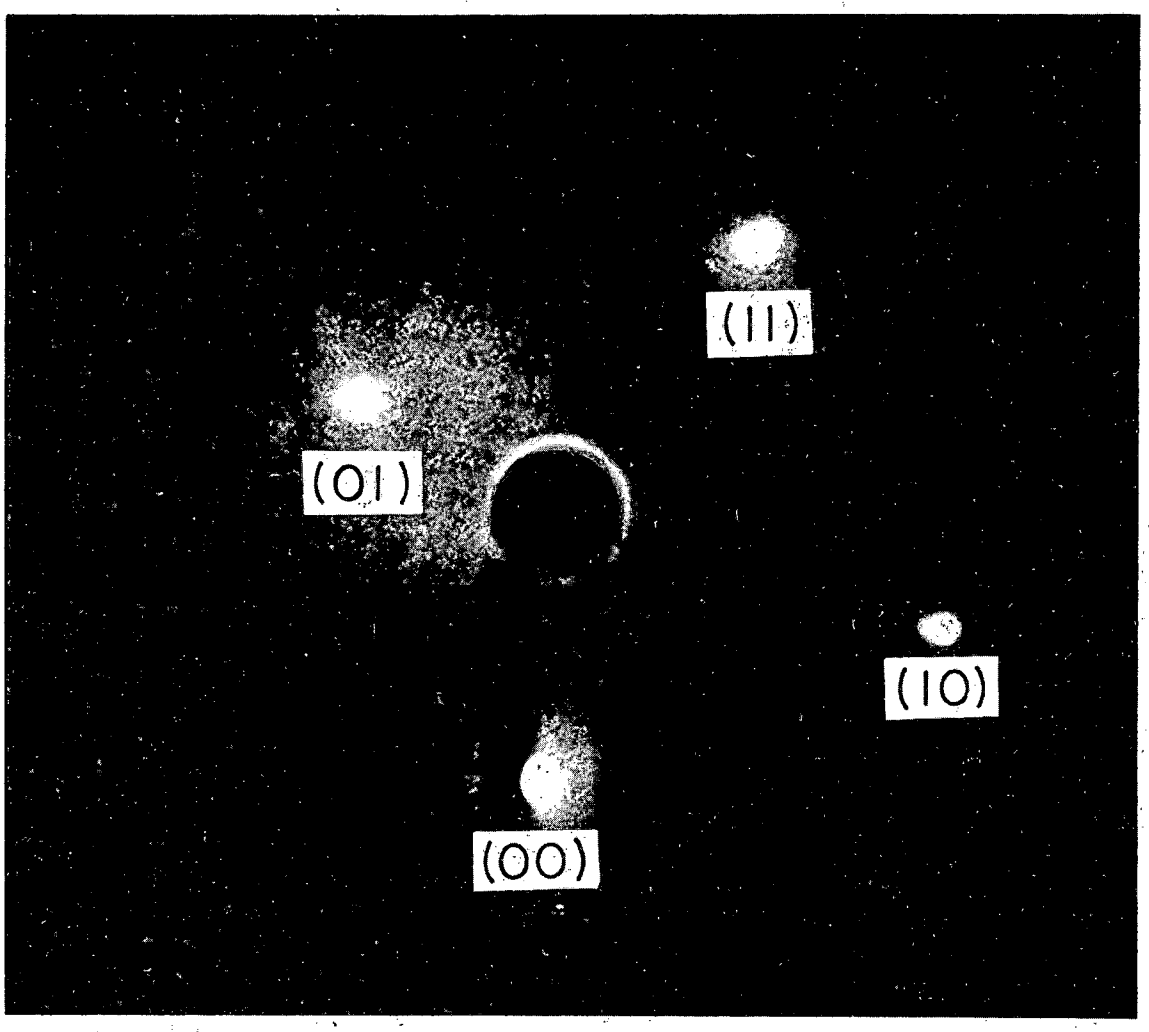

XBB 6812-7545

Fig. 14a

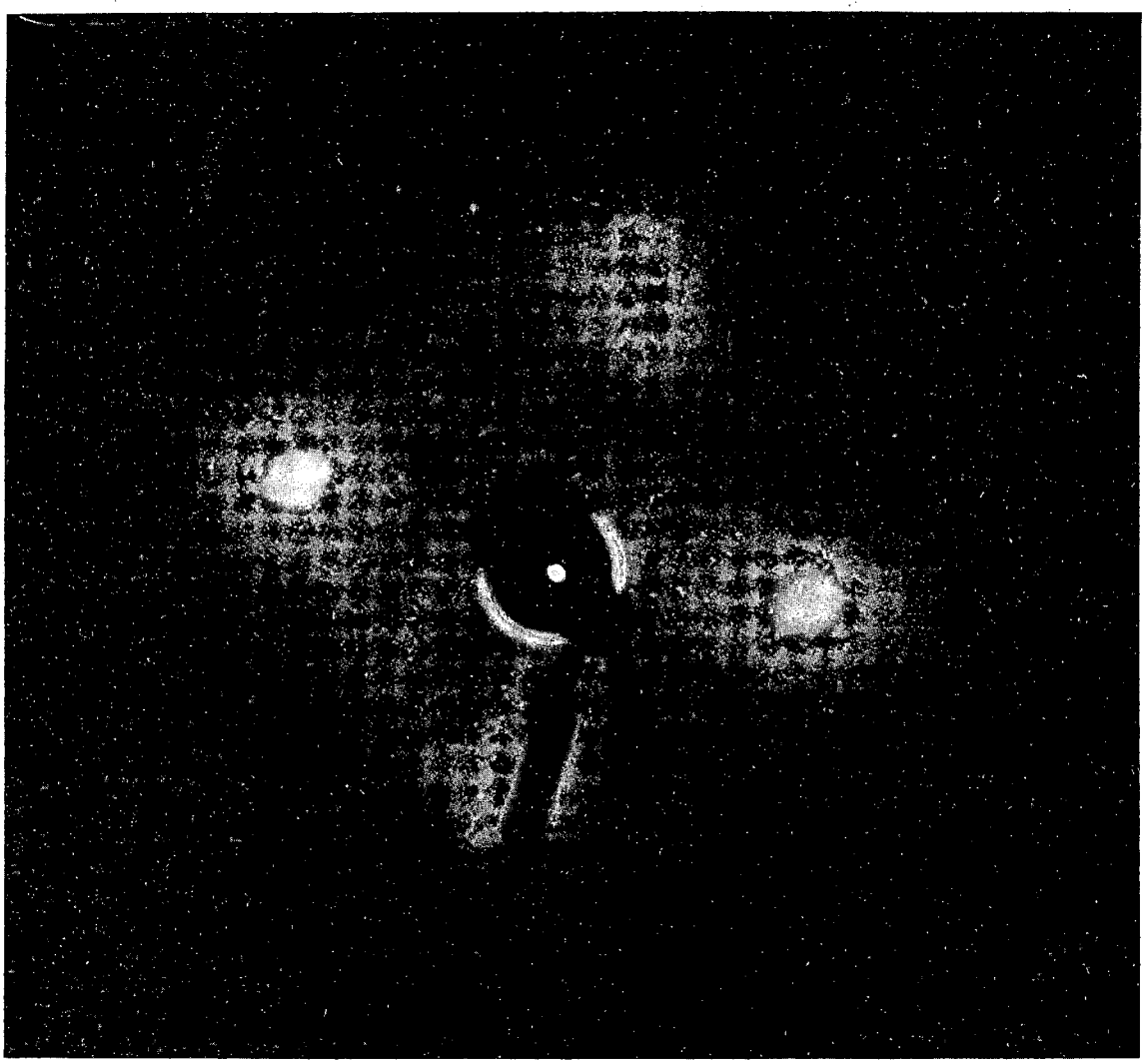

XBB 6812-7546

Fig. 14b

LEGAL NOTICE

This report was prepared as an account of Government sponsored work. Neither the United States, nor the Commission, nor any person acting on behalf of the Commission:

A. Makes any warranty or representation, expressed or implied, with respect to the accuracy, completeness, or usefulness of the information contained in this report, or that the use of any information, apparatus, method, or process disclosed in this report may not infringe privately owned rights; or

B. Assumes any liabilities with respect to the use of, or for damages resulting from the use of any information, apparatus, method, or process disclosed in this report.

As used in the above, "person acting on behalf of the Commission" includes any employee or contractor of the Commission, or employee of such contractor, to the extent that such employee or contractor of the Commission, or employee of such contractor prepares, disseminates, or provides access to, any information pursuant to his employment or contract with the Commission, or his employment with such contractor.

TECHNICAL INFORMATION DIVISION
LAWRENCE RADIATION LABORATORY
UNIVERSITY OF CALIFORNIA
BERKELEY, CALIFORNIA 94720